ISSN 0869-5911, Petrology, 2023, Vol. 31, No. 3, pp. 338–357. © Pleiades Publishing, Ltd., 2023.
Russian Text © The Author(s), 2023, published in Petrologiya, 2023, Vol. 31, No. 3, pp. 300–320.

Subduction and Oceanic Magmatism Records in Plutonic Rocks of the Kamchatsky Mys Ophiolite, Eastern Kamchatka

B. A. Bazylev[a], *, M. V. Portnyagin[b], D. P. Savelyev[c], G. V. Ledneva[d], and N. N. Kononkova[a]

[a] *Vernadsky Institute of Geochemistry and Analytical Chemistry, Russian Academy of Sciences, Moscow, Russia*
[b] *GEOMAR Helmholtz Centre for Ocean Research Kiel, Kiel, Germany*
[c] *Institute of Volcanology and Seismology, Far Eastern Branch, Russian Academy of Sciences, Petropavlovsk-Kamchatsky, Russia*
[d] *Geological Institute, Russian Academy of Sciences, Moscow, Russia*
**e-mail: bazylev@geokhi.ru*

Received May 24, 2022; revised October 25, 2022; accepted November 18, 2022

Abstract—The paper presents petrographic, mineralogical, and geochemical data on dunites, pyroxenites, peridotites, and gabbroids of the Kamchatsky Mys ophiolite. These data were acquired to distinguish cogenetic assemblages of igneous rocks, gain an insight into their geodynamic settings, and test various criteria of genetic links between the different magmatic rocks of ophiolites. The ultramafic and mafic rocks are shown to belong to two series, which differ in the compositions of the primary minerals, bulk rocks, and estimated trapped melts. The rocks of these series are found out to have been produced by geochemically different melts in different geodynamic settings, and during different episodes of mantle magmatism. The rocks of the high-Ti series (gabbro of the Olenegorsk massif, dunite and melanogabbro xenoliths in them, and vein gabbro in these xenoliths) crystallized from N-MORB melts in an oceanic spreading center. The rocks of the low-Ti series (dunite, pyroxenite, and gabbro veins in the residual spinel peridotites of the Mount Soldatskaya massif, as well as pyroxenite, peridotite, and gabbro alluvium and diluvium in the central and western parts of the peninsula) crystallized from water-rich boninite melts in relation to initial subduction magmatism. Taken into account the absence of boninite lavas from the Kamchatsky Mys ophiolite, the plutonic ultramafic rocks (including the rocks of the veins) might be the only evidence of subduction boninitic magmatism in the ophiolites. It was demonstrated that conclusions about the geodynamic settings of plutonic ultramafic and mafic rocks and recognition of cogenetic relations of these rocks with spatially associated basalts are more reliable when derived from the compositions of the trapped melts, which are estimated from their bulk geochemistry and primary mineral compositions, than when they are based on the mineral compositions only.

Keywords: ophiolites, dunite, pyroxenite, gabbro, boninite, N-MORB, Kamchatka
DOI: 10.1134/S0869591123030025

INTRODUCTION

Ophiolites are now viewed as fragments of variably disintegrated sections of the oceanic-type lithosphere produced in various parts of oceans: centers of oceanic, backarc, and forearc spreading; oceanic island arcs; regions with plume magmatism; etc. (Dilek, 2003; Dilek and Furnes, 2011). The most convincing evidence of the probable geodynamic environments in which ophiolite rocks have been formed are inferred from the geochemistry of the basalts (Dilek and Furnes, 2011), the composition of Cr-spinel phenocrysts from mafic and ultramafic volcanic rocks (Arai, 1992; Kamenetsky et al., 2001), primary minerals in residual peridotites (Dick and Bullen, 1984), and the geochemistry and bulk compositions of residual peridotites and clinopyroxene in them (Parkinson and Pearce, 1998). Mineralogical and geochemical features of plutonic mafic and, particularly, ultramafic rocks in ophiolites are much more rarely employed in petrological and geodynamic studies. This is explained, on the one hand, by the relatively scarce analytical data on such rocks in the modern oceanic lithosphere and, on the other, by the absence of reliable petrological–geochemical criteria for identifying geodynamic environments in which plutonic ultramafic and mafic rocks, first of all, their cumulus varieties, were formed.

The problem is that ophiolite complexes are often tectonically disintegrated, and the structure of the lithospheric sections whose fragments occur in the ophiolites is reproduced but not observed. Thereby it is commonly not analyzed whether the magmatic rocks (residual peridotites, plutonic ultramafic and mafic rocks, and basalts) are cogenetic in these reproduced sections. The problem of whether the plutonic and volcanic rocks are indeed cogenetic is particularly

severe in situations when geological relations suggest that the magmas were emplaced in a number of phases, whereas the geochemistry of the rocks and the chemistry of their primary minerals indicate that they were formed in different geodynamic environments. This is the case with, for example, the rock assemblage of the Kamchatsky Mys ophiolite, for whose various rock types (dominantly basalts and residual peridotites) petrological–geochemical arguments were presented of their origin in environments of mid-oceanic spreading, suprasubductional, and intraplate (Fedorchuk et al., 1989; Osipenko and Krylov, 2001; Kramer et al., 2001; Savelyev, 2003; Khotin and Shapiro, 2006; Tsukanov et al., 2007; Skolotnev et al., 2008; Portnyagin et al., 2008, 2009; Batanova et al., 2014).

This publication presents data on the mineralogy and geochemistry of the still-poorly studied nonresidual ultramafic and mafic rocks of the Kamchatsky Mys ophiolite to estimate the composition of the trapped melt of these rocks and compare these data with data on other rocks of this assemblage. Therewith our primary goal was to identify cogenetic assemblages among the magmatic rocks of the Kamchatsky Mys ophiolite and gain an insight into the geodynamic environments in which they were most probably produced. Our another goal was to test various criteria currently used to understand whether various magmatic rocks in ophiolite assemblages are cogenetic.

GEOLOGY

The ophiolite of the Afrika block in the southern part of the Kamchatsky Mys Peninsula, including the rocks we studied, occur in the modern junction region of the structures of the Kamchatka Peninsula and Aleutian Island Arc, which constrains the modern subduction zone beneath Kamchatka in the north. These ophiolites lie on the continuation of the structure of the Hawaii–Emperor Ridge and are thought to belong to the Kronotskii terrane and be a fragment of the accretionary prism of the ancient Kronotskii island arc. The latter was formed in the Late Cretaceous–Middle Eocene (Raznitsin et al., 1985; Zinkevich et al., 1993; Shcherbinina, 1997; Levashova et al., 2000; Tsukanov et al., 2014) in the Pacific at 36°–45° N (Khotin and Shapiro, 2006; Lander and Shapiro, 2007) and accreted to the Kamchatka margin in either the Late Eocene–Early Miocene (Zinkevich and Tsukanov, 1992; Alexeiev et al., 2006) or Late Miocene–Pliocene (Lander and Shapiro, 2007).

The Afrika block is made up of nappes (Fig. 1) and comprises the Mount Soldatskaya ultramafic massif, Olenegorsk gabbro massif, serpentinite mélange, Smaginskii association (Afrika complex, according to Tsukanov et al., 2007) of basalts with limestones and cherts with Aptian–Cenomanian fossils (Bragin et al., 1986; Fedorchuk et al., 1989), and the Pikezhskii tuff–chert association with Santonian–Turonian fossils (Bragin et al., 1986; Fedorchuk et al., 1989). The contacts between these structural units are mostly tectonic, and the Mount Soldatskaya and Olenegorsk massifs seem to be large nappes or their piles. The thick mélange zone contains fragments and relatively large blocks of pillow basalts, amphibolites, and ultramafic and gabbroic rocks.

The Mount Soldatskaya massif consists of mantle spinel harzburgites and rare spinel lherzolites, and the Olenegorsk massif is made up of various gabbroic rocks. This massif reportedly (Bethol'd et al., 1986; Khotin and Shapiro, 2006) includes continuous coherent sections from gabbro to dolerite and basalt, but it is hard to say how much accurately and realistically these sections have been reproduced.

The gabbroids of the Olenegorsk massif locally contain xenoliths of ultramafic rocks ranging from a few centimeters to 1 m. These xenoliths were interpreted (Vysotskii, 1986; Peyve, 1987; Kramer et al., 2001; Khotin and Shapiro, 2006) as residual spinel harzburgites, which are analogous to those of the Mount Soldatskaya massif but were variably intensely affected by reaction recrystallization. Earlier researchers have also documented schlieren and lens-shaped beds of ultramafic rocks in the eastern portion of the massif and in its southwestern part, in the lower reaches of the Vodopadnaya and Stremitel'naya rivers (Bethol'd et al., 1986; Kramer et al., 2001; Khotin and Shapiro, 2006). The gabbro reportedly hosts tectonic wedges of layered-complex rocks (alternating peridotites, plagioclase peridotites, olivine gabbroids, and anorthosites) (Kramer et al., 2001).

In the Mount Soldatskaya massif, nonresidual ultramafic rocks (dunites, clinopyroxenites, and websterites) make up rare lenses, veins, and tabular bodies in spinel peridotites (Osipenko and Krylov, 2001; Kramer et al., 2001; Khotin and Shapiro, 2006; Batanova et al., 2014), and the spinel peridotites of the massif also host veinlets of gabbroic rocks ranging from a few centimeters to 0.5 m in thickness.

Inasmuch as the technique for evaluating the composition of trapped melt was developed for dunites (Bazylev et al., 2019), we focused much attention on these rocks. No dunites have been known in the Olenegorsk massif, and hence, we studied the suite of melanocratic xenoliths in gabbro of this massif to identify dunites among these rocks. Our rock collection contains pyroxenite samples from the Mount Soldatskaya massif, which are centimeter-sized veinlets that cannot be utilized to study the geochemistry of the rocks. To bridge this gap, we studied the pyroxenites, peridotites that are close to them in containing high pyroxene contents, and melanocratic gabbroic rocks found as homogeneous rock blocks (up to 40 cm) in alluvium and diluvium in the western part of the

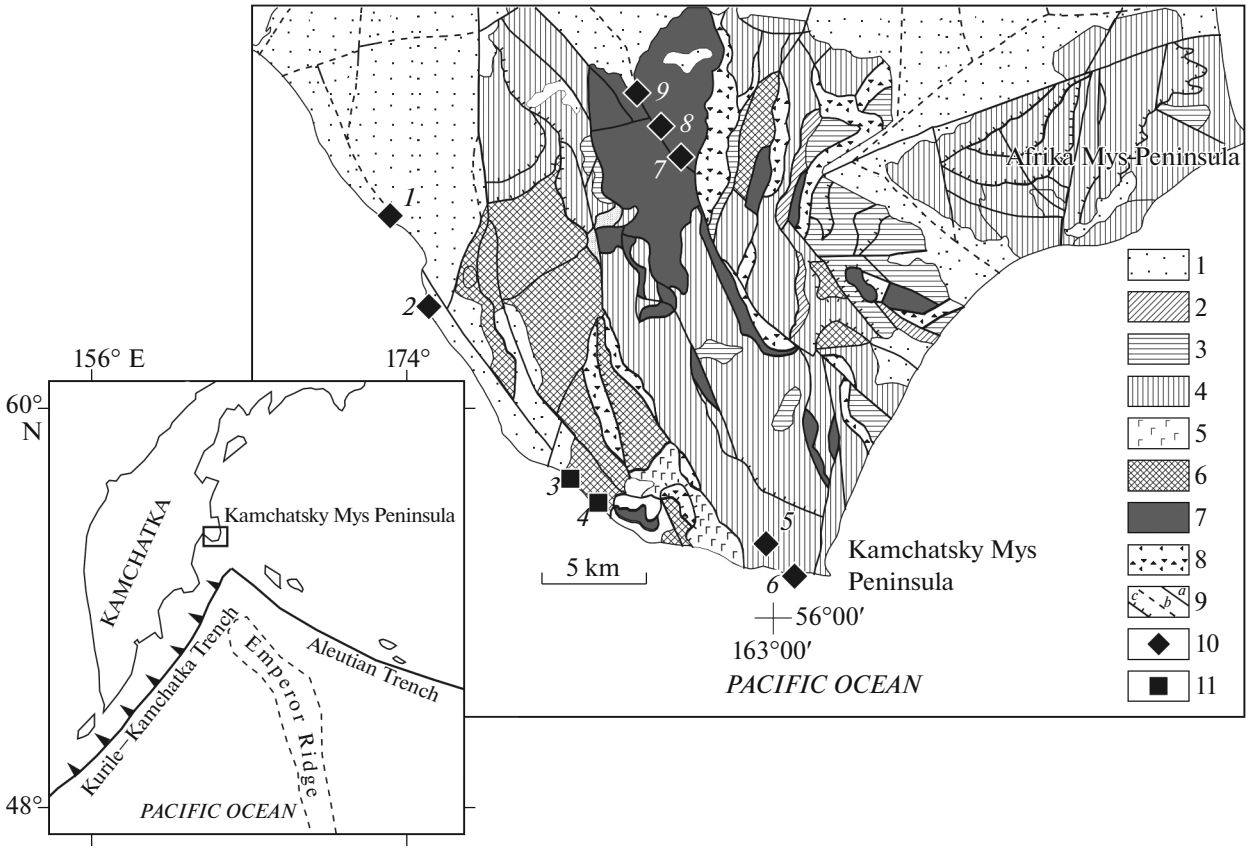

Fig. 1. Schematic geological map of the southern part of the Kamchatsky Mys Peninsula (modified from Boyarinova, 1999; Savelyev, 2003), showing the sampling sites. (1) Pliocene–Quaternary rocks; (2) Miocene terrigenous rocks; (3) Turonian–Campanian terrigenous rocks (Pikezhskaya Formation); (4) Albian–Cenomanian volcanic–chert rock sequences (Smaginskaya Formation); (5) pillow lavas classified with the Smaginskaya Formation in (Boyarinova, 1999) or Olenegorsk massif in (Khotin and Shapiro, 2006); (6) gabbro and dolerites of the Olenegorsk massif; (7) ultramafic rocks of the Mount Soldatskaya massif (the largest of the sampled blocks) and smaller bodies; (8) serpentine mélange; (9) faults: (*a*) observed, (*b*) inferred, overlain by loose rocks, (*c*) overthrusts; (10) ultramafic and gabbroic rocks of the low-Ti series; (11) ultramafic and gabbroic rocks of the high-Ti series. Numerals: (*1*) alluvium of the Mutnaya River (sample KM5-08), (*2*) alluvium of the Medvezh'ya River (samples KM5-01 and KM5-03), (*3*) bedrock outcrops and diluvium between the mouths of the Vodopadnaya and Stremitel'naya rivers (samples KM4-16, KM4-17, KM4-18, KM4-19, KM4-20a, KM4-22, and KM4-24), (*4*) alluvium of the Vodopadnaya River (samples KM4-12 and KM4-13), (*5*) alluvium of a stream southeast of the Kamennaya River (sample KM4-25), (*6*) diluvium on the southern shore near Kamennyi Gorodok (samples KM4-10 and KM4-11), (*7*) bedrock outcrop in the upper reaches of the Belaya River (sample KM4-28), (*8*) bedrock outcrop in the valley wall of the Belaya River (sample KM4-31), (*9*) alluvium of the Belaya River downstream of the Mount Soldatskaya massif (sample KM4-39v, KM5-17, KM5-18, KM5-19, KM5-22, and KM5-23).

Afrika block, along the shoreline of the western part of the peninsula, from the Medvezh'ya and Mutnaya rivers in the north to the southern tip of the peninsula, and from alluvium on the Belaya River downstream of the Mount Soldatskaya massif (Fig. 1), where these rocks occur together with dominant residual spinel peridotites analogous to those of the Mount Soldatskaya massif. This paper presents our results on gabbro from the Olenegorsk massif, ultramafic rocks and melanocratic gabbroids found as xenoliths in the gabbro, ultramafic rocks and gabbroids from veins in the spinel peridotites of the Mount Soldatskaya massif, and fragments of ultramafic rocks and melanocratic gabbroids from diluvium and alluvium in the western part of the Afrika block outside these massifs (Fig. 1).

METHODS

The samples were processed and prepared for their analysis at Vernadsky Institute of Geochemistry and Analytical Chemistry, Russian Academy of Sciences (GEOKHI RAS), in Moscow. Samples were crushed by a jaw crusher and powdered in mechanical grinders with agate mortars. The petrography of the rocks was studied in thin sections in transmitted and reflected light. The chemistries of minerals were analyzed at GEOKHI RAS on a Cameca SX100 microprobe at an accelerating voltage of 15 kV and current of 30 nA. The standards were standard reference samples of minerals provided by the Smithsonian Institution. The analyses were accurate to ±2 relative % at concentrations of 10–100 wt %, ±5 relative % at concentrations of 2–

10 wt %, ±10 relative % at concentrations of 1–2 wt %, and ±20 relative % at concentrations less than 1 wt %.

Rock samples were analyzed for major elements in pressed-powder pellets by XRF on a Phillips PW-1600 spectrometer at Vernadsky Institute. The tool was calibrated using nationally and internationally certified reference samples. The quality of the analyses was controlled by replicate analyses of internal standards.

Trace elements were analyzed by ICP-MS on a Finnigan Element XR mass spectrometer at the Institute of Geology of Ore Deposits, Petrography, Mineralogy, and Geochemistry, Russian Academy of Sciences (IGEM RAS), in Moscow. The samples were prepared by decomposing them in acids in a microwave oven. The accuracy of the analysis was controlled by systematically analyzing the BCR-2 internationally certified standard and internal standards. Concentrations of elements were calculated with the use of the ICP-MS-68A and HPS (A and B) standard solutions. The detection limits were 1–2 ng/g. The analytical errors of the analyses for REE in gabbro and pyroxenite was 5–10 relative % (1σ), and that in dunite (sample KM4-28) and harzburgite (sample KM4-31) was 35 relative % on average. The standard deviations in the concentrations of trace elements in the dunite (sample KM4-24, several replicate analyses) are listed in Suppl. 1, ESM_2.xlsx.

PETROGRAPHY AND MINERALOGY

The systematics of rocks in the text below and in Supplementary 1[1], ESM_1.xlsx is based on the calculated (Suppl. 1, ESM_2.xlsx, ESM_3.xlsx) or evaluated petrographic modal mineral composition of the rock protoliths according to (Le Bas and Streckeisen, 1991). The compositions of minerals are given in Suppl. 1, ESM_1.xlsx, ESM_6.xlsx; mineral symbols in the tables and figures are according to (Warr, 2021). Amphibole species are named according to the nomenclature (Hawthorne et al., 2012) and were calculated with the software (Locock, 2014).

Olenegorsk Massif

Xenoliths in the gabbro of the Olenegorsk massif. Based on petrographic and mineralogical studies of xenoliths hosted in the gabbroic rocks (Fig. 2a), these xenoliths are classified into two groups: residual spinel harzburgites, which were described in much detail in previous studies and are not discussed below, and presumably cumulus ultramafic rocks, which are discussed in this publication.

The ultramafic and mafic rocks of the xenoliths are dunite (sample KM4-24), plagioclase–clinopyroxene dunite (sample KM4-22), and melanocratic olivine gabbronorite (samples KM4-13 and KM4-19). The rocks are variably (from moderately to almost completely) altered. The replacements of primary minerals are usually pseudomorphic, with relics of the primary minerals preserved in some of the pseudomorphs. Most of the rocks are massive, coarse-grained, and hypidiomorphic-granular (the only exception is sample KM4-13, which is banded, with alternating melanocratic and leucocratic layers, Fig. 2b). The silicate grains are typically 1–3 mm, occasionally up to 7 mm.

The Cr-spinel grains are opaque, euhedral, are large in the dunites (up to 1 mm) and smaller in the gabbroids (no larger than 0.3 mm), and this mineral also occurs as inclusions in the olivine and clinopyroxene and along boundaries of silicate grains (Figs. 2c–2f). The olivine is intensely to completely replaced by serpentine. Clinopyroxene grains in the dunites are up to 1.5 mm, mostly anhedral, and are replaced by brownish bastite with abundant dust of ore minerals along cleavage planes (Figs. 2c, 2d). In the olivine gabbronorite (sample KM4-13), large anhedral clinopyroxene grains host roundish euhedral olivine inclusions (Fig. 2f), and the rock locally acquires a poikilitic texture. Plagioclase forms anhedral grains up to 1–1.5 mm (Fig. 2d) in the dunites and subhedral ones, as large as 6 mm, and their aggregates in the gabbronorites. The plagioclase is replaced by finely scaly optically isotropic or finely tabular weakly anisotropic colorless chlorite (Fig. 2d), pumpellyite, thompsonite, and vuagnatite in the dunites and mostly by prehnite in the gabbroic rocks (Fig. 2f). In contrast to the bastite pseudomorphs after clinopyroxene (Figs. 2c, 2e), the pseudomorphs after plagioclase do not contain inclusions of ore mineral (Fig. 2e), which makes it easy to reliably distinguish between them. The amount of the relatively large bastite pseudomorphs after clinopyroxene in the dunite of sample KM4-24 is no greater than the amount of the Cr-spinel, and no pseudomorphs after plagioclase were identified in this sample (below we will explain why this fact is important and is emphasized here).

The Cr-spinel of the samples has Cr# = Cr/(Cr + Al) = 0.40–0.59, contains 0.3–2.7 wt % TiO_2, and has F# = Fe^{3+}/(Cr + Al + Fe^{3+}) = 0.11–0.20. The minerals of most of the rocks are fairly homogeneous in composition, and appreciable variations were found only in the Cr# and TiO_2 concentration of the Cr-spinel. Samples KM4-19 and KM4-22 were found out to contain Cr-spinel grains of much higher Mg# and elevated *F*#, as is typical of metamorphic populations of this mineral. The Mg# = 100Mg/(Mg + Fe) of olivine

[1] Supplementary materials for the Russian and English versions of this paper at https://elibrary.ru/ and http://link.springer.com/, respectively, are presented in Supplementary 1:
ESM_1.xlsx: rock compositions;
ESM_2.xlsx: bulk and modal mineral compositions of the rocks;
ESM_3.xlsx: comparison of the measured rock compositions and those calculated from the compositions of the minerals and mineral modes;
ESM_4.xlsx: mineral/melt partition coefficients of elements;
ESM_5.xlsx: evaluated concentrations and compositions of melts entrapped in the rocks;
ESM_6.xlsx: compositions of the secondary silicate minerals.

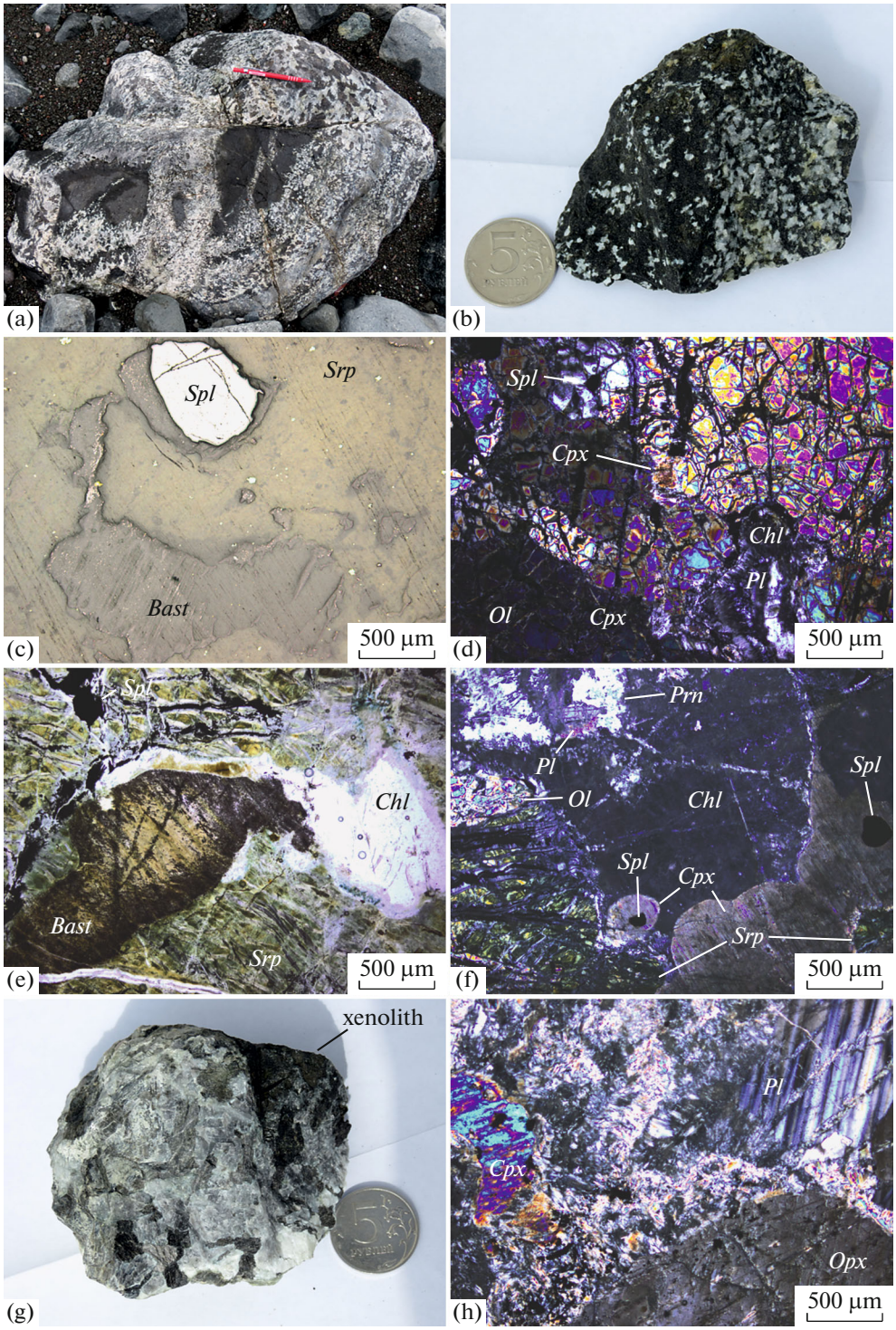

Fig. 2. Rocks of the Olenegorsk massif. (a) Xenoliths of ultramafic rocks and melanocratic gabbroids; (b) xenolith of banded olivine gabbronorite (sample KM4-13); (c) Cr-spinel and bastite replacing clinopyroxene in serpentinized dunite (sample KM4-24), in reflected-light; (d) Cr-spinel, clinopyroxene, and plagioclase (relic in the central part of a chlorite preudomorph) grains in dunite (sample KM4-22), in cross-polarized light (CPL); (e) Cr-spinel in replaced olivine (mesh serpentine), bastite replacing clinopyroxene, and a chlorite pseudomorph after plagioclase in olivine norite (sample KM4-19), in plane-polarized light (PPL); (f) clinopyroxene with Cr-spinel and olivine inclusions, partly serpentinized olivine, and replaced plagioclase with a relic (sample KM4-13), CPL; (g) hornblende gabbronorite (sample KM4-20a) with a xenolith fragment; (h) grains of pyroxenes and plagioclase intensely replaced by prehnite (sample KM4-20a), CPL.

in the rocks is 89.1–86.0, and the mineral contains 0.31–0.23 wt % NiO. The clinopyroxene has Mg# = 88.0–88.9 and contains 0.8–1.0 wt % TiO_2, 3.3–3.7 wt % Al_2O_3, and 0.4–0.6 wt % Na_2O. Single small grains of magnesian hornblende were found as roundish inclusions in clinopyroxene of the olivine gabbro and are rich in TiO_2 (3.0 wt %) at relatively low K_2O concentrations. The plagioclase relics found in two samples correspond to bytownite ($An_{81–82}$). These rocks contain no orthopyroxene relics.

Gabbroid veinlets in the xenoliths. Some of the xenoliths host gabbro veinlets 0.5–1.5 cm thick (samples KM4-17v, KM4-20v), and some of the diluvium blocks consist of an ultramafic rock in one-side contact with gabbroid (the thicknesses of the gabbroids are 1–3 cm). The latter (samples KM4-16g and KM4-18g) can be either rocks that host the xenoliths or veinlets cutting across them. The plagioclase of these rocks is completely replaced, no orthopyroxene has been found in the rocks, and the clinopyroxene is noted for elevated Mg# = 86.1–92.3 and, in some samples, elevated Cr_2O_3 concentrations (up to 1.1 wt %). At the same time, the Al_2O_3 concentration of the mineral varies relatively little (2.7–3.1 wt %), as also does the TiO_2 concentration (0.34–1.04 wt %). The rock of sample KM4-17v contains preserved relics of magnesian hornblende, which is rich in TiO_2 (2.3–2.6 wt %) at relatively low K_2O concentrations, variable Mg#, Al_2O_3 and Cr_2O_3 concentrations. The rock also contains small ilmenite grains.

Gabbro hosting the xenoliths. The rock hosting the xenoliths is hornblende gabbronorite (sample KM4-20a), which is a massive coarse-grained rock, with mineral grains typically ranging from 1 to 6 mm (Fig. 2g). The plagioclase and clinopyroxene grains are equant, the clinopyroxene is somewhat more subhedral than the plagioclase. The clinopyroxene is pretty fresh, whereas the plagioclase is extensively replaced by prehnite, pectolite, chlorite, and thompsonite. The plagioclase relics are polysynthetically twinned. The large orthopyroxene grains (Fig. 2h) and the margins of the clinopyroxene grains are replaced by greenish magnesian hornblende. The rock contains anhedral grains of brownish and greenish hornblende and rare small (no larger than 0.2 mm) anhedral ilmenite grains but neither olivine nor Cr-spinel.

The Mg# of the clinopyroxene varies from 79.2 in the cores of grains to 74.9 in their rims and in small grains. The clinopyroxene contains (wt %) TiO_2 0.7–0.9, Al_2O_3 ~2.9, Cr_2O_3 0.1–0.4, and Na_2O ~0.4. The Mg# of the orthopyroxene also varies, from 77.6 to 72.6, and the mineral is relatively rich in TiO_2 (0.3–0.5 wt %) at a moderate Al_2O_3 concentration (1.5 wt %). The relict plagioclase is labradorite ($An_{63–58}$). The anhedral hornblende (pargasite) is rich in Al_2O_3 at relatively low TiO_2 and K_2O concentrations, which likely indicates that the hornblende has partially recrystallized in the subsolidus.

Mount Soldatskaya Massif

The veins studied in the clinopyroxene-bearing spinel peridotites are made up of a broad rock spectrum (Fig. 3a–3f), ranging from dunite (samples KM4-28 and KM5-23) and clinopyroxene-free harzburgite (sample KM4-31) to olivine websterite (samples KM5-18v and KM4-19v) and gabbronorite (samples KM5-17v, KM4-39v, and KM4-12mv). These rocks are usually moderately altered. The rocks are massive, coarse-grained, hypidiomorphic-granular or pegmatoid in sample KM4-39v. Cr-spinel grains in the rocks are opaque, small, and euhedral. The olivine grains reach 3 mm. Orthopyroxene grains in the dunites and harzburgites are about 0.5 mm and are occasionally as large as 2 mm, anhedral or, more rarely, roundish, and are intensely replaced by tremolite. Sample KM5-23 contains close to 2% olivine (Fig. 3b), and sample KM4-31 contains about 10% of this mineral. No clinopyroxene grains were found in these dunites and harzburgites.

In the samples of the olivine websterites (sample KM5-18v, a veinlet about 1 cm thick, and sample KM5-19v, a veinlet thicker than 3 cm), large (up to 6 mm) pyroxene grains are surrounded by fine-grained aggregates of pyroxene with olivine. The contacts between the veinlets and host harzburgites are smooth and sharp (Fig. 3d).

The norite (?) of sample KM5-17v (veinlet 2–3 cm thick) contains preserved large (up to 12 mm) equant orthopyroxene grains in a groundmass of plagioclase and clinopyroxene, which are completely replaced by prehnite and actinolite. Clinopyroxene is preserved only as small round inclusions in orthopyroxene. A thin veinlet in gabbronorite (?), sample KM4-12mv, contains clinopyroxene grains with inclusions of pleochroic hornblende.

The hornblende gabbronorite, sample KM4-39v, from a veinlet about 5 cm thick in harzburgite (Fig. 3f) is a pegmatoid rock, whose primary minerals are intensely replaced, with their relics preserved only in the central portions of the grains. The pyroxenes are replaced mostly by green amphibole and Al-free diopside, whereas the plagioclase is replaced by chlorite, pectolite, vuagnatite, and an optically isotropic mineral of the sodalite group (it is white in hand-specimens).

Cr-spinel in the dunites and harzburgites is very rich in Cr (Cr# = 0.82–0.90), its Fe is relatively little oxidized (F# = 0.022–0.033), and the mineral is very poor in TiO_2 (0.02–0.05 wt %). No Cr-spinel has been found in either the websterites or the gabbroic rocks. Olivine in the dunites and harzburgites is highly magnesian (Mg# = 91.1–92.2) and is rich in NiO (0.35–0.42 wt %), whereas olivine in the websterites has Mg#

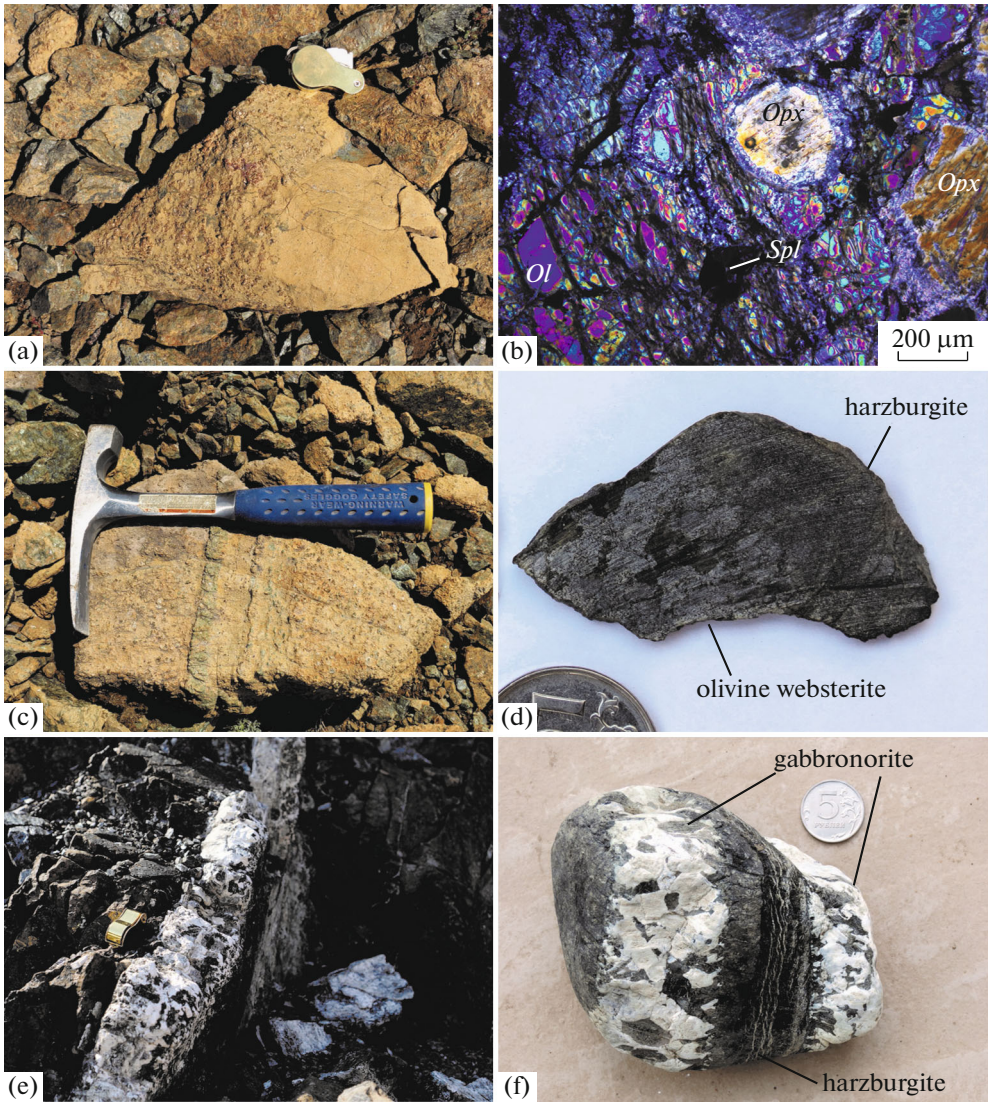

Fig. 3. Vein rocks in harzburgites of the Mount Soldatskaya massif. (a) Contact between dunite (right) and harzburgite; (b) Cr-spinel and orthopyroxene grains in dunite (sample KM5-23), CPL; (c) pyroxenite veinlets in harzburgite; (d) contact between olivine websterite (sample KM5-19v) and host harzburgite; (e) pegmatoid gabbroid vein in harzburgite; (f) hornblende gabbronorite veinlets (sample KM4-39v) in harzburgite.

lower than 88.8. Orthopyroxene in the dunites and harzburgites has high Mg# = 91.6–91.9 and is very poor in Al_2O_3 (0.23–0.34 wt %) and CaO (0.5–0.8 wt %). It should be mentioned that the studied harzburgite, sample KM4-31, is principally different from the typical residual spinel harzburgites of the Mount Soldatskaya massif in composition of Cr-spinel and orthopyroxene but is close to the dunite. Orthopyroxene from the websterites has a lower Mg# (80–89) and is richer in Al_2O_3 (0.9–1.3 wt %). Orthopyroxene in the gabbroids is even less magnesian (63–81) at the same levels of Al_2O_3 and CaO concentrations. Clinopyroxene has high Mg# = 92.4–86.3 in the websterites and lower Mg# = 85.1–66.9 in the gabbroids. Clinopyroxene in all of the rocks is poor in Al_2O_3 (0.7–1.7 wt %), TiO_2 (0.02–0.24 wt %), and Na_2O (0.12–0.37 wt %). Brown hornblende (pargasite) in gabbronorite sample KM4-12v is high in Al_2O_3 (10.1 wt %), TiO_2 (2.1 wt %), and K_2O (0.5 wt %) and is definitely primary magmatic. Brown hornblende (magnesian–ferric hornblende) in gabbronorite sample KM4-39v is rich in TiO_2 (1.2 wt %) and also seems to be primary magmatic. Plagioclase is preserved in a single sample and is in it very calcic: An_{96}.

Ultramafic and Mafic Rocks in Diluvium and Alluvium in the Western Part of the Afrika Block

The samples examined in the course of this study are dominated by websterites, some of which contain

plagioclase (or pseudomorphs after it) and hornblende. Sample KM4-25 is plagioclase–hornblende harzburgite, sample KM4-10 is plagioclase-bearing lherzolite, and sample KM4-11 is melanocratic olivine–hornblende norite. Unlike all of the vein pyroxenites described above, all of these rocks contain accessory Cr-spinel. Most of the rocks are dominantly massive (only sample KM4-10 shows discernible banding, with linear pyroxene segregations), inequigranular, coarse-grained to medium-grained (Figs. 4a, 4b), hypidiomorphic-granular, porphyritic, or more rarely poikilitic. Samples KM5-03 and KM4-11 (Fig. 4b) contain linear veinlets of leucocratic olivine-free gabbronorite (samples KM5-03v and KM4-11v), 0.5 and 1.5 cm thick, respectively. In a veinlet in sample KM5-03v, all primary mafic minerals are replaced by fine-grained aggregates of metamorphic minerals, mostly by greenish amphibole, and only plagioclase grains with polysynthetic twins, up to 6 mm across, are preserved. A veinlet of hornblende gabbronorite in sample KM4-11v consists of plagioclase (45%), orthopyroxene (25%), poikilitic brown hornblende (20%), clinopyroxene (5%), and magnetite (2%) (Fig. 4h).

Cr-spinel occurs in the rocks as small (no larger than 0.1–0.2 mm) opaque euhedral grains, mostly inclusions in olivine and clinopyroxene or, more rarely, in orthopyroxene. The veinlets are devoid of Cr-spinel grains. The olivine grains are up to 6 mm. If the rocks contain more than 30% of this mineral, its grains are euhedral roundish (Fig. 4b), whereas the olivine-poor rocks contain it in the form of anhedral grains. The large (3–10 mm) equant clinopyroxene grains host small orthopyroxene lamellas (Fig. 4c), roundish inclusions of olivine (Fig. 4d) and orthopyroxene (up to 0.8 mm), and small (no larger than 0.2 mm) anhedral or more rare euhedral hornblende inclusions. Clinopyroxene in some of the rocks is intensely replaced by amphibole (Fig. 4d), with this process associated with the development of tremolite or actinolite and local recrystallization of the primary into alumina-free diopside. Large (3–7 mm) orthopyroxene grains in these rocks are more anhedral and sometimes host roundish inclusions of olivine (Fig. 4e) and clinopyroxene, and are poikilitic in some rocks. The orthopyroxene is replaced by tremolite, actinolite, and bastite. The hornblende usually occurs as anhedral grains up to 0.8 mm at contacts between olivine and pyroxenes and as roundish inclusions (up to 0.2 mm) in the clinopyroxene and, more rarely, orthopyroxene. If the rock is rich in hornblende, the latter forms large (up to 10 mm) poikilitic grains with roundish pyroxene and olivine inclusions (Figs. 4e, 4f) and aggregates of anhedral grains in the intergranular space between grains of other silicates. In the large poikilitic grains, their brown color is particularly deep in their central portions, whereas hornblende in the margins is paler, greenish to colorless (Fig. 4f). In two samples with the most magnesian silicates (samples KM5-22 and KM5-01), neither plagioclase nor pseudomorphs after it were found. In most of the other samples, plagioclase grains (or chlorite–prehnite pseudomorphs after them) are as large as to 0.5 mm and anhedral (Fig. 4g). In the rocks with elevated plagioclase contents (samples KM4-25 and KM4-11), its grains reach 1.5 mm and occasionally up to 5–6 mm, plagioclase in these rocks is replaced dominantly by prehnite, and round inclusions in it are usually completely replaced. Magnetite in a veinlet in sample KM4-11v forms anhedral grains up to 0.3 mm in close association with the primary silicates (Fig. 4h), and some of the magnetite grains host thin ilmenite platelets.

Spinel in the samples has Cr# = 0.52–0.80, contains 0.11–0.44 wt % TiO_2, and is characterized by a degree of Fe oxidation of 0.10–0.26. All grains studied in some of the rocks are similar in composition, whereas spinel grains in the other samples show remarkable variations in both Cr# and degree of Fe oxidation. The compositional variations within single grains (cores to rims) are much smaller than the aforementioned variations between the grains. Samples KM4-10 and KM5-03 contain Cr-spinel grains with lower MgO concentrations and with a significantly elevated degree of Fe oxidation of 0.31–0.39. These grains are likely metamorphic.

The olivine has Mg# = 90.8–83.0 and shows variations in NiO concentrations (mostly 0.21–0.34 wt %). In some of the rocks, large pyroxene grains are zoned: their Al_2O_3 concentration increases and Mg# decreases from cores to rims, and the composition of the marginal parts of the large grains corresponds to that of the smaller grains. The clinopyroxene contains (wt %) TiO_2 0.03–0.10, Al_2O_3 0.8–2.3, and Na_2O 0.14–0.31 and has Mg# = 94.0–86.4. The orthopyroxene has Mg# = 90.7–83.4 and contains 1.1–2.1 wt % Al_2O_3. The hornblende (pargasite, magnesiohastingsite, and more rare magnesian hornblende) has Mg# = 89.7–82.5 and contains 10.3–12 wt % Al_2O_3. Along with hornblende relatively rich in TiO_2 and rich in K_2O (up to 0.6 wt % TiO_2 and up to 0.7 wt % K_2O), the same rock samples and sometimes even the same grains contain hornblende with lower TiO_2 and K_2O concentrations (mostly magnesian hornblende). Plagioclase in the preserved relics in sample KM4-10 is bytownite (An_{82}), similar to plagioclase in the veinlet in sample KM5-03v (An_{88}).

In sample KM4-11, in the outer contact of a veinlet (sample KM4-11c), the Mg# of the silicates decreases only insignificantly, and this parameter increases in the inner contact of the veinlet (sample KM4-11vc), where the orthopyroxene and hornblende contain slightly more Ti, particularly in the central part of the veinlet (sample KM4-11v), where the silicates have the lowest Mg# = 79.8 for the clinopyroxene, 73.8 for the orthopyroxene, and 71.3 for the hornblende, and the hornblende is the richest in TiO_2 (2.0 wt %). The composition of the plagioclase varies from An_{69} in the margin of the veinlet to An_{58} in its central part. Magnetite in the veinlet broadly varies in concentrations of Cr_2O_3, Al_2O_3, and TiO_2.

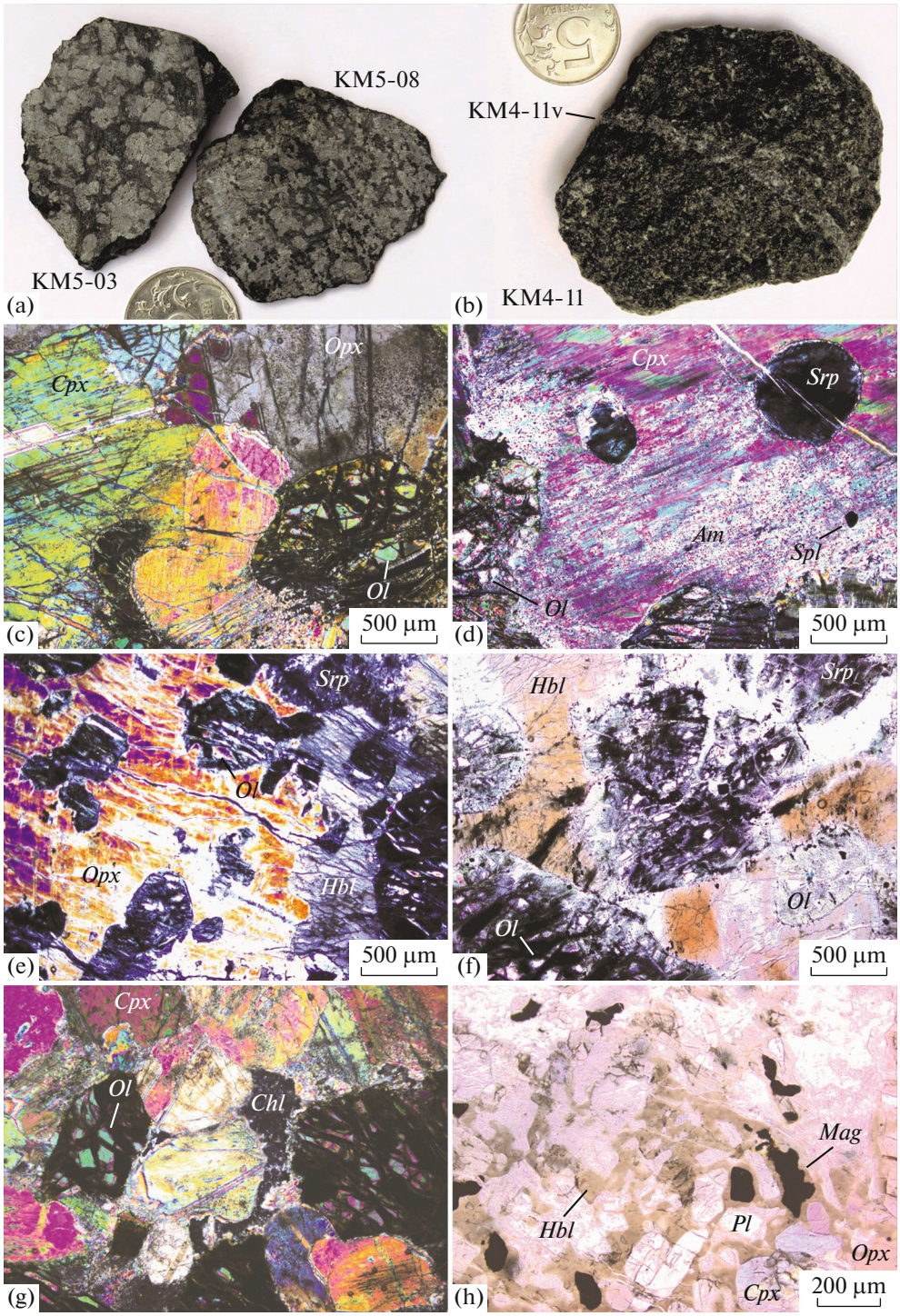

Fig. 4. Cumulus ultramafic and mafic rocks from the alluvium and diluvium. (a) Olivine websterite, pyroxenite (pale), and partly serpentinized olivine (dark); (b) hornblende norite veinlet (sample KM4-11v) in olivine–hornblende gabbronorite (sample KM4-11); (c) typical texture of the olivine websterite (sample KM5-08), CPL; (d) euhedral inclusions of olivine (which is completely replaced by serpentine) and Cr-spinel in clinopyroxene, which is partly amphibolized (sample KM5-01, olivine websterite), CPL; (e) poikilitic orthopyroxene and hornblende grains with euhedral olivine inclusions (sample KM4-25, plagioclase–hornblende harzburgite), CPL; (f) poikilitic grain of heterogeneous hornblende with olivine inclusions (sample KM4-25), PPL; (g) chlorite pseudomorph after an anhedral plagioclase grain (sample KM5-08), CPL; (h) poikilitic hornblende grain with pyroxene, plagioclase, and magnetite inclusions (sample KM4-11v), PPL.

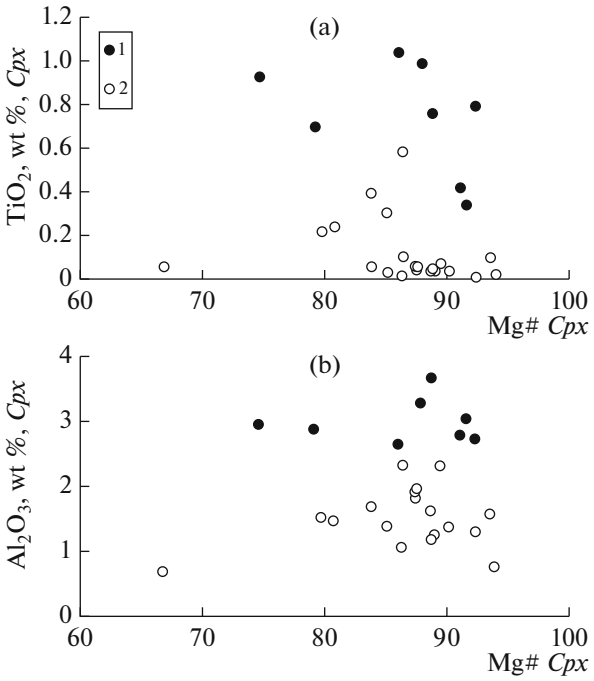

Fig. 5. Concentrations of (a) TiO_2 and (b) Al_2O_3 in clinopyroxene in rocks of different ultramafic series of the Kamchatsky Mys. (1) High-Ti series; (2) low-Ti series.

SERIES OF PLUTONIC ULTRAMAFIC–MAFIC ROCKS

Based on the composition of their primary minerals and typical mineral assemblages, the studied ultramafic and mafic plutonic rocks are classified into two series, which can be referred to as high-Ti and low-Ti ones (Figs. 5, 6).

The rocks of the **high-Ti series** are the gabbroic rocks of the Olenegorsk massif, xenoliths of cumulus ultramafic and melanocratic mafic rocks in these gabbro, and gabbro veinlets cutting across these xenoliths. Clinopyroxene in the rocks of this series typically contains mildly elevated Al_2O_3 concentrations (2.7–3.7 wt %) and elevated TiO_2 ones (0.34–1.0 wt %), which are consistent with data on the mineralogy of the gabbro in (Kramer et al., 2001) (no whole analyses of the minerals have been published). According to the amphibole geobarometer (Ridolfi et al., 2010), the rocks crystallized at 2–3 kbar, and the oxygen fugacity was therewith evaluated at QFM + 2.0 to QFM + 2.7 by the oxygeobarometer (Ballhaus et al., 1991).

The relations between the Cr# = 0.40–0.60 of the spinel and its TiO_2 concentration (0.32–2.7 wt %) indicate that the high-Ti rocks are definitely different from dunites, pyroxenites, and gabbroids related to arc (suprasubductional) geodynamic settings of magmatism (Arai et al., 2011) but are close to analogous rocks in mid-oceanic ridges (MORs) (Fig. 6) and hotspots (these rocks are undistinguishable in terms of these parameters).

The rocks of the **low-Ti series** are the dunites, websterites, and gabbroic rocks in veins in the spinel peridotites of the Mount Soldatskaya massif and the ultramafic and mafic rocks sampled in the alluvium and diluvium in the western part of the peninsula. The latter can be interpreted as probable fragments of bodies in the residual spinel peridotites. Some features of the rocks from the diluvium and alluvium, such as directional and banded structures, poikilitic textures, and the occurrence of cutting gabbroid veinlets and accessory Cr-spinel, are atypical of vein rocks but typical of cumulus rocks in relatively large bodies. Clinopyroxene in the rocks of this series is characterized by low

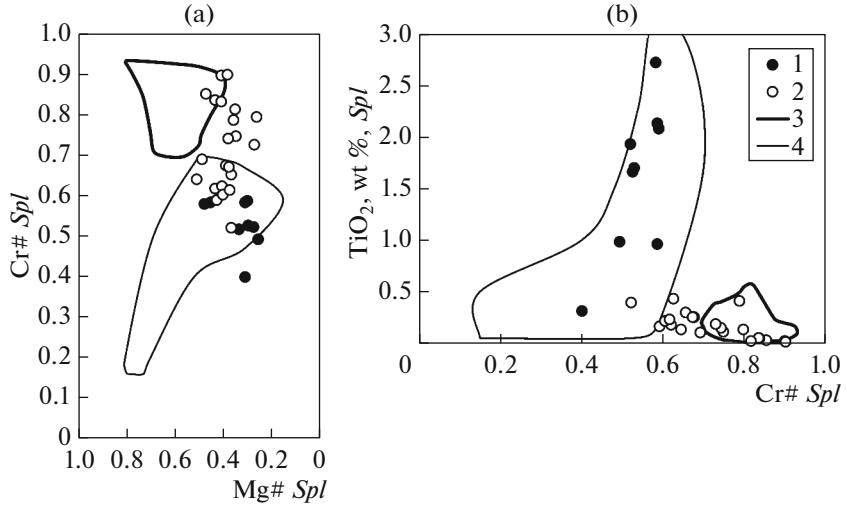

Fig. 6. Compositions of Cr-spinel in rocks of (1) the high-Ti series and (2) low-Ti series. The composition fields of Cr-spinel (3) from boninites is according to (Sobolev and Danyushevsky, 1994), and (4) from non-residual ultramafic rocks and gabbroids in MOR is according to (Arai et al., 2011).

Al_2O_3 concentrations (0.7–2.3 wt %) and very low TiO_2 ones (0.01–0.24 wt %). According to the amphibole geobarometer (Ridolfi et al., 2010), the rocks crystallized at 1–3 kbar. The oxygen fugacity, which was evaluated by the olivine–orthopyroxene–spinel geobarometer, was QFM – 0.6 to QFM + 0.1 for the dunites and harzburgites and QFM + 1.1 to QFM + 2.6 for the rest of the rocks.

The relations between the Cr# of the spinel (0.52–0.90) and its TiO_2 concentration (0.02–0.44 wt %) indicate that the rocks of the low-Ti series undoubtedly correspond to dunites, pyroxenites, and gabbroids related to arc geodynamic environments of magmatism (Arai et al., 2011), with the very high Cr# values of spinel in the dunites, considered together with indications that the orthopyroxene crystallized after the olivine and Cr-spinel, make it possible to parallel this mineral with that in boninites (Fig. 6).

The petrography of the rocks and their typical metamorphic minerals (Suppl. 1, ESM_6.xlsx) indicate that the rocks of both series were metamorphosed under *P–T* parameters corresponding to the amphibolite, greenschist, prehnite–pumpellyite, and zeolite metamorphic facies. The rocks provide no evidence of their contact or prograde metamorphism, or high-pressure/low-temperature metamorphism, as well as no evidence of their rodingitization (the rocks contain no calcic garnet, hydrogranate, and vesuvianite). The metamorphism was likely retrograde and occurred at least partly during the disintegration of the lithosphere, when slices of mantle and crustal rocks were tectonically combined. Mineralogical data indicate that allochemical (with undoubted potassium introduction) metamorphism could have affected only the hornblende gabbronorite of sample KM4-39v, in which plagioclase of anorthite composition is intensely replaced by pectolite and a sodalite-group mineral (Suppl. 1, ESM_1.xlsx, ESM_6.xlsx).

GEOCHEMISTRY AND MODAL MINERAL COMPOSITION OF THE ROCKS

The bulk compositions of the rocks are presented in Suppl. 1, ESM_2.xlsx, and their normalized multielemental patterns are displayed in Fig. 7.

The low concentrations (at the level of those in the primitive mantle and lower) of incompatible elements of the rocks are typical of cumulus ultramafic and mafic rocks. This suggests that the bulk compositions of the rocks were controlled by the contents and compositions of the cumulus phases and the contents and compositions of the intercumulus melt, which is referred to as *trapped melt* in petrological papers. Upon the crystallization of melts trapped in plutonic rocks, partial or complete reequilibration was reached between the compositions of the cumulus and intercumulus phases. The dunites and harzburgites are noted for relatively low concentrations of the rare-earth elements (REE), which are controlled by the modal composition of the rocks, but the diagram shows that the rocks of the low- and high-Ti series cannot be unambiguously distinguished from one another.

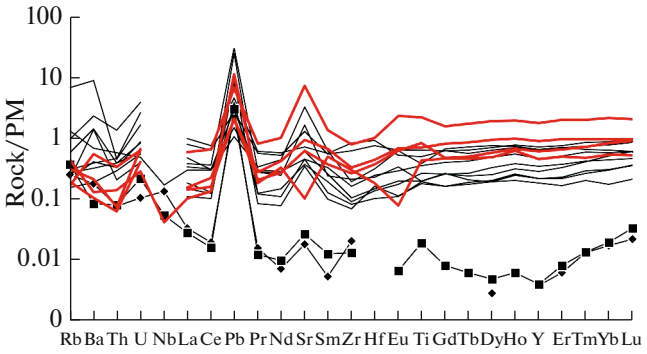

Fig. 7. Primitive mantle-normalized (Sun and McDonough, 1989) patterns of incompatible elements for the rocks of the high-Ti series (heavy red lines) and low-Ti series (thin lines; the dunite and harzburgite compositions—symbols).

To evaluate the modal proportion of primary minerals in the rocks, we applied the technique of mass-balance calculations based on the bulk compositions of the rocks and the compositions of their primary minerals, with the aggregate squared relative errors minimized between the analyzed and calculated compositions of the rocks. If some primary mineral, or minerals, are completely replaced, we used the composition of this mineral (or minerals) from another, most suitable sample.

The results of these calculations (which can be found in Suppl. 1, ESM_3.xlsx) indicate that the alterations of most of the samples were isochemical, Na and, more rarely, other elements were introduced into or removed from some of the samples, and these elements were excluded from the calculations.

For sample KM4-19, which does not contain preserved relics of primary silicates, the Mg# of these minerals was evaluated, under the assumptions that Fe and Mg were inert at metamorphism, from general correlations between the Mg# of the coexisting silicates in the ultramafic–mafic plutonic rocks. The Mg# was evaluated at 80.7 for the olivine, 82.3 for the orthopyroxene, and 85.3 for the clinopyroxene.

The modal mineral composition of dunite sample KM4-24, which is practically completely serpentinized and whose alterations were associated with significant changes in concentrations of major components, was evaluated based on petrographic data, which indicate that this rock contained cumulus clinopyroxene in an amount no higher than that of Cr-spinel.

The calculated modal mineral compositions of the rocks are listed in Suppl. 1, ESM_3.xlsx. They are generally consistent with the petrography of these rocks, although the calculated contents of orthopyroxene in

the olivine gabbroids of the high-Ti series (in which practically no orthopyroxene was found) seems to be overestimated because of the partial removal of Ca from these rocks. The presence of dunite (as well as harzburgite with low-Al orthopyroxene) in both the low- and the high-Ti series allowed us to evaluate their contents of trapped melts and the compositions of the latter and then to carry out analogous estimations for the other rocks.

EVALUATION OF THE CONTENT AND COMPOSITION OF TRAPPED MELT IN THE DUNITES

In a mass-balance equation, the concentration of element *i* in a rock can be expressed as the sum of the concentrations of this element in phases composing this rock, including the trapped melts (*tm*) (Bédard, 1994). For example, for the studied rocks

$$C_i^{\text{rock}} = (\varphi^{Ol} C_i^{Ol}) + (\varphi^{Spl} C_i^{Spl}) + (\varphi^{Opx} C_i^{Opx}) + (\varphi^{Cpx} C_i^{Cpx}) + (\varphi^{Pl} C_i^{Pl}) + (\varphi^{\text{tm}} C_i^{\text{liq}}), \quad (1)$$

where φ is the mass fraction of a phase in the cumulus mineral association (corrected for the content of trapped melt), and *C* is the concentration (in wt %) of element *i* in the bulk composition of the rock and its various phases. In the absence of data on the concentration of element *i* in a mineral and with regard to that

$$C_i^{\text{Min}} = C_i^{\text{liq}} D_i^{\text{Min-liq}}, \quad (2)$$

Eq. (1) can be rewritten in the form

$$C_i^{\text{liq}} = C_i^{\text{rock}} \Big/ (\varphi^{Ol} D_i^{Ol-\text{liq}} + \varphi^{Spl} D_i^{Spl-\text{liq}} + \varphi^{Opx} D_i^{Opx-\text{liq}} + \varphi^{Cpx} D_i^{Cpx-\text{liq}} + \varphi^{Pl} D_i^{Pl-\text{liq}} + \varphi^{\text{tm}}), \quad (3)$$

which enables one to evaluate the concentrations of trace elements and REE in the trapped melt from data on the mineral–melt partition coefficients D_i, the modal mineral composition of the protolith of the rocks (which approximately reflects the composition of the cumulus without hornblende), and the evaluated amount of the trapped melt.

The dependence for the content of trapped melt applicable to pyroxene-free dunite (Bazylev et al., 2019) is

$$\varphi^{\text{tm}} C_i^{\text{liq}} = C_{Al_2O_3}^{\text{rock}} - C_{Cr_2O_3}^{\text{rock}} \left(C_{Al_2O_3}^{Spl} \Big/ C_{Cr_2O_3}^{Spl} \right), \quad (4)$$

and that for pyroxene-bearing dunite acquires the form

$$\varphi^{\text{tm}} C_i^{liq} = C_{Al_2O_3}^{\text{rock}} - (C_{Cr_2O_3}^{\text{rock}} - \varphi^{Opx} C_{Cr_2O_3}^{Opx} - \varphi^{Cpx} C_{Cr_2O_3}^{Cpx})(C_{Al_2O_3}^{Spl} \Big/ C_{Cr_2O_3}^{Spl}) - \varphi^{Opx} C_{Al_2O_3}^{Opx} - \varphi^{Cpx} C_{Al_2O_3}^{Cpx}. \quad (5)$$

To estimate the probable phase proportions in the cumulus, we subtracted hornblende (which obviously crystallized from the trapped melt or was produced by reactions between this melt with cumulus minerals) from the modal mineral composition of the rocks and normalized the contents of the remaining phases to 100%. This resulted in a certain error (because some amounts of the pyroxenes and plagioclase also crystallized from the trapped melt, i.e., belong to the intercumulus, as also follows from that hornblende occurs as inclusions in the pyroxene), but these errors are insignificant if the trapped melt contents are small.

In the instance of dunite sample KM4-24, the calculations done for equal clinopyroxene and Cr-spinel contents (1.1% *Cpx* and 1.1% *Spl*), and for clinopyroxene content, which is twice lower than that of spinel (0.6% *Cpx* and 1.2% *Spl*), yield practically identical concentrations of the trapped melt (4.6% and 4.7%, respectively). The content of trapped melt in the dunite, sample KM4-28, was 1.3%, and that in the harzburgite, sample KM4-31, was evaluated at 1.0% by Eq. (5).

Concentrations of incompatible elements in the trapped melts were calculated with the use of mineral/melt partition coefficients for plagioclase and clinopyroxene from (Zajacz and Halter, 2007; Bédard, 2006), for orthopyroxene from (Frei et al., 2009) (experimental run 1101-12-06), and for olivine compiled from (Bazylev et al., 2019) (Suppl. 1, ESM_4.xlsx). The calculated composition of the melt trapped in the dunite of the high-Ti series is close to the composition of N-MORB, and that of the dunite and harzburgite of the low-Ti series is close to boninite-type melt (Suppl. 1, ESM_5.xlsx), which is consistent with the compositions of the primary spinel in these rocks.

EVALUATION OF THE AMOUNTS OF INTERCUMULUS MELT TRAPPED IN THE ULTRAMAFIC ROCKS AND GABBROIDS

This technique for evaluating the content of trapped melts is inapplicable to rocks with high pyroxene concentrations and to plagioclase-bearing varieties. In these situations, the composition of the intercumulus melt trapped in the pyroxenites can be approximately evaluated under the assumption that the melt content was 1–2% (Varfalvy et al., 1997; Ledneva et al., 2017), which often leads to realistic and interpretable melt compositions. Another approach in evaluating the composition of trapped (intercumulus) melt in cumulus gabbroic rocks (Perk et al, 2007; Berger et al., 2017) and pyroxenites (Tamura and Arai, 2006; Batanova et al., 2011; Karimov et al., 2020) is

based on data on the geochemistry of the primary minerals and the use of mineral/melt partition coefficients. The assumption of fractional crystallization of the melts makes it possible to estimate the amount of the trapped melt (Perk et al, 2007; Berger et al., 2017). However, even in the absence of data on the geochemistry of the primary minerals, the amount of melt trapped in pyroxenites and gabbroids can in principle be evaluated if the massifs contain, along with these rocks, also dunites cogenetic with them, which seems to be the case with our rocks.

At the fractional crystallization of melt, concentrations of incompatible elements in this melt correlate with the Mg# of the equilibrium silicates, with this parameter reflecting the progress in crystallization differentiation. Both of these parameters can be modeled if the probable composition of the parental melt and crystallized parameters are specified.

According to the calculations done for the dunites and harzburgites, the probable parental melt of the rocks of the high-Ti series was assumed to have had a composition as those of the most primitive melt inclusions in MOR basalts (Sobolev and Shaussidon, 1996), and that of the rocks of the low-Ti series have corresponded to the composition of the upper pillow lavas of the Troodos massif (sample VPL-1b and VPL-2; Portnyagin, 1997) calculated from data on olivine-hosted melt inclusions and the estimated compositions of the parental melts of boninites in the Tonga Trench, of the eastern (EG) and western (WG) groups (Sobolev and Danyushevsky, 1994). The simulations were carried out with the COMAGMAT ver. 3.74 software (Ariskin and Barmina, 2004). The crystallization of the melts was simulated at 2 kbar and oxygen fugacity corresponding to the QFM buffer. Variations in the pressure up to 4 kbar and oxygen fugacity up to QFM + 1.5 practically do not any significantly modify the relations between the geochemistry of the melt and the Mg# of the equilibrium silicates within the range of oxygen fugacity values calculated for our samples. The simulations were carried out with the mineral/melt partition coefficients mentioned above.

Concentrations of the most incompatible elements in the rocks are the most susceptible to the amount of the trapped melt, but Rb, Ba, and U may be mobile when rocks are altered, and the Th and Nb concentrations of dunites are analyzed with relatively large errors, which makes La the optimal element for such calculations. The concentration of this element in the dunite, considered together with the Mg# of the olivine (1.44 ppm La in melt in equilibrium with olivine with Mg# 89.1 for the high-Ti series; and 1.81 ppm La in melt in equilibrium with olivine with Mg# 91.7 for the low-Ti series) serves as a benchmark for evaluating the level of La concentrations in the more evolved melts.

In the strict sense, the Mg# of silicates in cumulus rocks somewhat differs from the probable Mg# of silicates in the cumulus association of these rocks at the equilibrium temperature with the melt (this parameter of cumulus phases can initially vary and undergo changes at reequilibration with the trapped melt and intercumulus generations of minerals under subsolidus conditions).

The fractional crystallization mechanism of melts surmised for the origin of cumulus ultramafic and gabbroic rocks (Perk et al, 2007; Berger et al., 2017) may, perhaps, be complicated for the vein dunites, gabbroids, and pyroxenites by the partial reequilibration of the melts with host rocks, their partial assimilation, and mixing of melts of different composition (Varfalvy et al., 1997; Tamura and Arai, 2006; Batanova et al., 2011; Karimov et al., 2020). However, the petrography of the rocks indicates that not all of our samples can be reasonably reliably classified with vein rocks, it is difficult to quantitatively evaluate the effects of the aforementioned phenomena and processes, and this can be neglected when rough provisional estimates are carried out.

With the application of this approach, the content of trapped melt in the pyroxenites and gabbroic rocks can be evaluated in diagrams, as is illustrated by the example of some rocks of the high-Ti series in Fig. 8 and by rocks of the low-Ti series in Fig. 9. As obviously seen in the diagrams, the estimates conducted using various minerals of a single sample are in good mutual agreement, and the variations in the Mg# of the silicates within ± 2 to ± 3 mol % usually do not any principally affect the estimated contents of trapped melts. For the high-Ti series, the range of the trapped melt contents is relatively narrow: 3–8% for the rocks of the low-Ti series and is impressively broad for those of the high-Ti series (0.8–31%), but it is still comparable to, for example, the range of estimates for the gabbroids of the Iguilid mafic intrusion in the West African Craton, Mauritania (Berger et al., 2017).

ESTIMATION OF THE COMPOSITION OF THE MELTS TRAPPED IN THE ULTRAMAFIC AND GABBROIC ROCKS

The estimated content of melt trapped in the ultramafic and gabbroic rocks makes it possible to calculate, using Eq. (3), concentrations of incompatible elements in the melts trapped by the rocks (Suppl. 1, ESM_4.xlsx).

The calculated compositions of melts trapped by rocks of the high-Ti series are similar, correspond to the compositions of depleted tholeiitic basalts of the Kamchatsky Mys, and are comparable to the compositions calculated from data on olivine-hosted melt inclusions in picrites from the Kamchatsky Mys (Fig. 10). The negative Eu anomaly of the dunite-trapped melt may indicate that plagioclase crystallized from this melt (although the rock contains no this mineral). The high

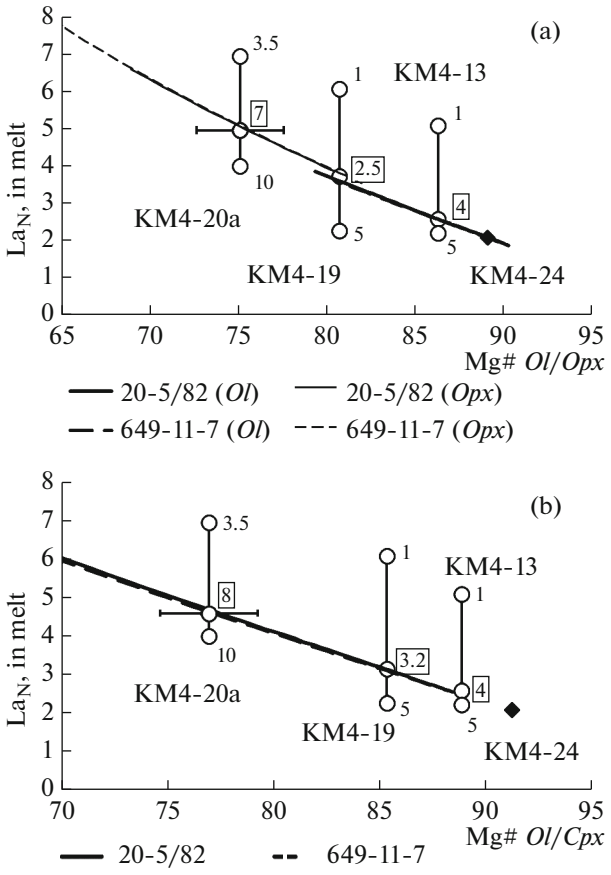

Fig. 8. Evaluated contents of the trapped melt in rocks of the high-Ti series. For each sample, La concentrations were calculated in the trapped melt (normalized to the composition of the primitive mantle according to Sun and McDonough, 1989) depending on the specified content of trapped melt (1–10 wt %, numerals without boxes); the probable concentrations of the trapped melt (numerals in boxes) were evaluated from their consistency with the fractional crystallization trend of the assumed parental melt (samples 20-5/82 and 649-11-7 from Sobolev and Shaussidon, 1996) relative to the Mg# of (a) the olivine (or orthopyroxene for sample KM4-20a) and (b) clinopyroxene.

positive Pb anomaly is most likely explained by its introduction at alterations of the rocks. As has been established by comparing the compositions of the altered and unaltered melt inclusions in Cr-spinel in basalts from the Kamchatsky Mys, the alterations of the rocks proceed at a mobile behavior of Ba, U, and Sr (Portnyagin et al., 2009). The broad variations in the concentrations of these elements and Pb in tholeiites and basalts from the Kamchatsky Mys (Fig. 10) confirm this and provide evidence that the elements were likely mobile during the alterations of the rocks, and the concentrations of these elements in the calculated melt compositions (and the Pb concentration as well) may reflect not so much the composition of the trapped melt as the degree of the mobility of these elements during the rock alterations. Bearing this in mind and taking into account the general similarities in the calculated compositions of the trapped melts and backarc-basin basalts (BABB), it is reasonable to believe that the trapped melts may correspond to the compositions of both BABB and N-MORB.

The calculated compositions of the trapped melts in the rocks of the low-Ti series (Fig. 11) exhibit typical features of boninite-type melts: low to very low MREE and HREE concentrations, U-shaped configurations of the REE patterns, notably elevated Ba, U, and Sr concentrations, and the absence of clearly discernible Nb anomalies. Similar to the melts trapped by the rocks of the high-Ti series, the calculated Rb, Ba, Pb, and Sr in these melts (for at least some of the rocks) may reflect the mobile behavior of these elements at the rock alterations. However, the degrees of alterations of the rocks of the low-Ti series are notably lower than those of most rocks of the high-Ti series, and the calculated modal mineral compositions of these rocks indicate that major components (Na inclusive) remained inert at the alterations of most of these rocks. This led us to admit that concentrations of these elements in the melts of at least some of the rocks may correspond to the real ones. The significant variations in the concentrations of MREE and HREE in the melts may have resulted from deviations of the differentiation mechanisms of the melts from fractional crystallization, as well as some differences in the compositions of the parental melts. In any event, these melts cannot be viewed as produced by the fractional crystallization of a single parental melt, and they were most probably formed by the fractionation of a series of similar melts (with the obvious introduction of mobile elements from rocks of the subducted slab), which differ in the degree of melting of the mantle source. This result is not surprising with regard to the fact that the ultramafic and mafic rocks of this series were sampled from widely spaced outcrops but not within a single massif.

DISCUSSION

Probable Geodynamic Setting of the Origin of the Rocks of the High-Ti Series

Cr-spinel in the rocks of the high-Ti series with high TiO_2 concentrations (0.3–2.7 wt %), mildly elevated Cr# (0.40–0.59), and elevated degree of Fe oxidation (Fe^{2+}/Fe^{3+} = 1.9–2.7) plots within the overlap area of the composition fields of Cr-spinel cumulus ultramafic and mafic rocks in MAR and hotspots (intraplate ocean environments) (Arai et al., 2011). For example, most of these spinels are analogous to olivine-hosted spinel inclusions in Hawaiian basalts, which contain 1.1–3.3 wt % TiO_2, have Cr# = 0.49–0.73 and Fe^{2+}/Fe^{3+} = 1.2–2.7 (Sobolev and Nikogosyan, 1994) and correspond to typical magmatic spinel in olivine-hosted inclusions in oceanic-island basalts (OIB) (Kamenetsky et al., 2001) (although the com-

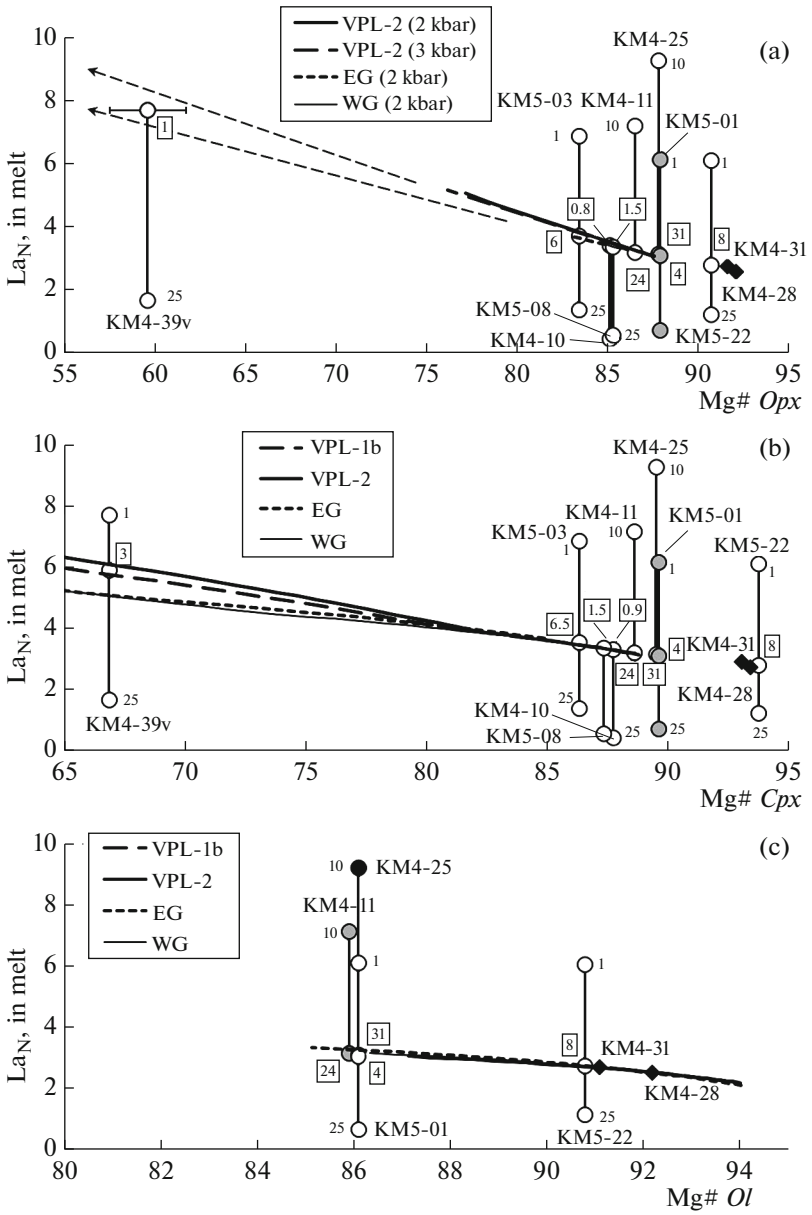

Fig. 9. Evaluated amounts of melt trapped in the rocks of the low-Ti series. For each sample, La concentrations in the trapped melt are calculated (the values are normalized to the composition of the primitive mantle according to Sun and McDonough, 1989) depending on the specified content of trapped melt (0.8–31 wt %, numerals without boxes); the probable contents of trapped melt (numerals in boxes) are evaluated from their consistency with the trend of fractional crystallization of the assumed parental melt (VPL-1b and VPL-2 from Portnyagin, 1997; EG and WG from Sobolev and Danyushevsky, 1994) relative to the Mg# of (a) the orthopyroxene, (b) clinopyroxene, and (c) olivine. The trends of Mg# of orthopyroxene in the course of crystallization are extrapolated (arrows).

positions of spinel from the plutonic rocks show systematic differences from the compositions of spinel from the cogenetic volcanics; Arai, 1992; Arai et al., 2011).

The relatively late crystallization of orthopyroxene (after clinopyroxene and plagioclase) in the rocks of this series is typical of both tholeiites and more alkaline (intraplate) melts. The low hornblende contents in the rocks provide evidence of low water contents in the parental melts.

The mineralogy of the rocks thus does not offer any definite clues to understand the environments in which the ultramafic and mafic rocks of the high-Ti series (Olenegorsk massif) were formed but makes it possible to constrain the circle of the environments to MOR and intraplate oceanic ones. However, the calculated compositions of the trapped melts in these rocks display no evidence of their intraplate origin. These melts are characterized by weakly depleted REE patterns at their relatively high concentrations, as is

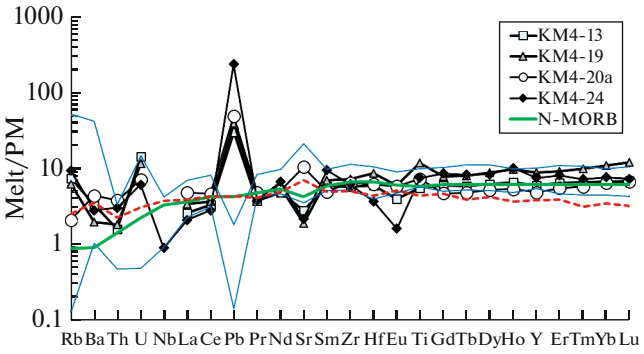

Fig. 10. Calculated primitive mantle-normalized multielemental patterns of melts trapped in the rocks of the high-Ti series in comparison with the composition of tholeiites and N-MORB-type basalts of the Kamchatsky Mys (Tsukanov et al., 2007; Duggen et al., 2007; Portnyagin et al., 2009) (the variation limits in the concentrations of elements are shown with thin lines without symbols), with the average composition of the melts calculated using melt inclusions in olivine from the picrites of the Kamchatsky Mys (Korneeva et al., 2020) (red dashed line), and with the composition of N-MORB (Sun and McDonough, 1989).

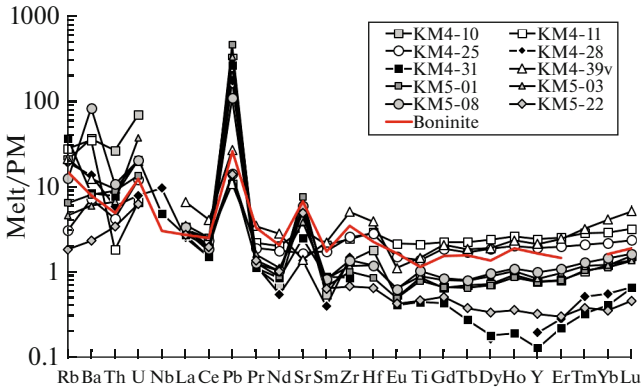

Fig. 11. Calculated primitive mantle-normalized multielemental patterns of the rocks of the low-Ti series in comparison with the average composition of boninite (Kelemen et al., 2003). Solid symbols are the compositions of melts trapped by the dunite and harzburgite, gray symbols are such compositions for the plagioclase-free and low-plagioclase pyroxenites and peridotite, and the open symbols are those for the gabbroids and peridotite rich in plagioclase.

typical of melts of the N-MORB and BABB types. The calculated compositions of the melts trapped in the rocks of the high-Ti series fairly well correspond (in terms of concentrations of immobile elements) to the compositions of basalts of the N-MORB type in the Smaginskaya Formation and the average composition of melt inclusions in olivine in picrites from the Kamchatsky Mys (Fig. 10). The range of the Cr# (0.40–0.59) of spinel in them is close to that of spinel from depleted tholeiites (N-MORB) of the Smaginskaya Formation in the Kamchatsky Mys: 0.32–0.52 (Portnyagin et al., 2009). Considered together with data on the composition of the minerals and the high probability that strongly incompatible elements mobile in fluids have been redistributed (see above), this led us to give preference to the crystallization of the ultramafic and mafic rocks of the high-Ti series from tholeiitic melts of the N-MORB type. The good consistency of the multielemental patterns of all rocks of this series, from dunite to gabbro, suggests that all of them crystallized from a single partial melt.

The facts and considerations presented above led us to think that the basalts (of the N-MORB type) of the Smaginskaya Formation of the Kamchatsky Mys are probable comagmates of the plutonic ultramafic rocks of the high-Ti series (Olenegorsk massif) and to believe that these rocks make up a complex that was produced at an oceanic spreading center, as was suggested in (Portnyagin et al., 2006; Khotin and Shapiro, 2006). The $^{40}Ar/^{39}Ar$ age of the depleted olivine–plagioclase tholeiites, dikes, and gabbroids (~95 Ma, Cenomanian) (Portnyagin et al., 2006) falls within the age range when the Smaginskaya rock assemblage was formed (in the Aptian–Cenomanian according to paleontological evidence) (Bragin et al., 1986; Fedorchuk et al., 1989).

The higher (than is typical of mid-oceanic ridges) degree of melting of the mantle source, which was inferred for both the residual peridotites of the Mount Soldatskaya massif (Batanova et al., 2014) and the melt inclusions in olivine from picrites in the Kamchatsky Mys (Nekrylov et al., 2021), which was interpreted as following from the proximity of a hotspot (plume) to the oceanic spreading center, in which these rocks were likely formed (Portnyagin et al., 2008, 2009; Batanova et al., 2014), considered together with the complementary character of the Sr anomaly in the melts (which is positive; Portnyagin et al., 2009; Korneeva et al., 2020) and clinopyroxene in the residual peridotites (which is negative; Batanova et al., 2014), suggest that the Albian–Cenomanian volcanic rocks of the Kamchatsky Mys are cogenetic with the mantle spinel peridotites in the Mount Soldatskaya massif (Nekrylov et al., 2021).

This is inconsistent with the hypothesis that the gabbro of the Olenegorsk massif was produced in a suprasubductional environment (at a backarc or intra-arc spreading center) (Tsukanov et al., 2007).

Probable Geodynamic Setting of the Origin of the Low-Ti Series

The high Cr# (0.82–0.90) of spinel in the dunites and harzburgite from the Mount Soldatskaya massif unambiguously indicates that the rocks were formed by suprasubductional boninite magmatism, as was hypothesized in (Osipenko and Krylov, 2001). However, the relations of the pyroxenites and gabbroids of this series, which contain spinel with lower Cr#, to

boninite magmatism is not obvious and is reliably supported only by some compositional features of the primary Cr-spinel (Fig. 6) and the geochemistry of the trapped melts (Fig. 11). With regard to that the Cr# of spinel is different in the dunites (0.82–0.90) and the rest of the ultramafic and mafic rocks of this series (0.52–0.80), and to the difference between the degrees of Fe oxidation, it is reasonable to suggest that the parental melts of these rocks were somewhat different in composition, as also follows from the calculated compositions of the trapped melts. Nevertheless, all Cr-spinel in the rocks of the low-Ti series shows Al_2O_3 to TiO_2 proportions typical of Cr-spinel in olivine-hosted inclusions in arc magmas (Kamenetsky et al., 2001), and the low TiO_2 concentrations in spinel in most of the rocks corresponds to that in the parental magmas of boninites. In diagrams of the composition of spinel from plutonic rocks, the data points of spinel from our rocks of the low-Ti series also plot within the field of arc rocks (Arai et al., 2011).

The early crystallization of orthopyroxene in the rocks of this series (before clinopyroxene and plagioclase crystallization) and the intercumulus association, which involves hornblende, correspond to the crystallization sequence of minerals in water-rich melts of the boninite type under relatively low pressures. A relatively low pressure of their crystallization also follows from the relatively low alumina concentrations in the pyroxenes found in association with olivine and plagioclase.

The composition of clinopyroxene from a pyroxenite dike cutting the harzburgites of the Mount Soldatskaya massif (1.11 wt % Al_2O_3, 0.10 wt % Na_2O) and the composition of spinel in this pyroxenite (Cr# = 0.68, 0.05 wt % TiO_2) (Kramer et al., 2001) indicate that this pyroxenite is close to the pyroxenites of the low-Ti series. The composition of clinopyroxene in gabbroids from the tectonic block studied in the upper reaches of the First Ol'khovaya River (Kramer et al., 2001; Tsukanov et al., 2007) are also similar to the composition of clinopyroxene in the rocks of the low-Ti series.

In the absence of geochronologic data on the ultramafic and mafic rocks of the low-Ti series, it is reasonable to suggest that the age of suprasubductional magmatism, including boninite one, in the Kamchatsky Mys corresponds to the magmatic zircon age of the plagiogranites that cut across the gabbroids of the block in the upper reaches of the First Ol'khovaya River: 74.7 ± 1.8 Ma (Campanian) (Luchitskaya et al., 2006). This corresponds to the time when the intraoceanic Kronotskaya island arc started to develop (the ophiolite assemblage of the Kamchatsky Mys ophiolite is thought to be a fragment of the accretionary wedge of this arc) in the Coniacian–Campanian (Zinkevich and Tsukanov, 1992). In principle, boninite magmatism is typical of the early development of island-arc systems, and the absence of volcanic tholeiite and boninite rocks of this age among the Kamchatsky Mys rocks may be explained by the low intensity of the suprasubductional magmatism in the forearc basin (Hawkins, 2003) and/or by that this magmatism occurred mostly in the plutonic mode; a still another probable explanation is that the rocks have been eroded.

Our data presented above led us to suggest that suprasubductional ultramafic and gabbroic rocks in the Kamchatsky Mys ophiolite do not occur only in the relatively small block in the upper reaches of the First Ol'khovaya River (Kramer et al., 2001; Tsukanov et al., 2007), as was hypothesized in (Khotin and Shapiro, 2006), but are spread practically over the whole field of this complex.

Lately more and more petrological and geochemical lines of evidence were retrieved that the vein dunites and pyroxenites in the residual peridotites of ophiolite complexes are formed by suprasubductional melts of the boninite type (Varfalvi et al., 1997; Tamura and Arai, 2006; Batanova et al., 2011; Ledneva et al., 2017; Bazylev et al., 2019; Karimov et al., 2020). Thereby no boninites have ever been found in some of these complexes, as in that of the Kamchatsky Mys, so that the plutonic ultramafic rocks, including their vein varieties, may turn out to be the only evidence of the boninite magmatic episode of the processes that have produced these complexes.

CONCLUSIONS

1. Plutonic ultramafic–mafic rocks of the Kamchatsky Mys ophiolite complex affiliate with two genetic series, which differ from each other in the composition of their primary minerals, the modal mineralogy of the rocks, and the calculated compositions of the trapped melts. These series correspond to different episodes of mantle magmatism in different geodynamic environments.

2. The mafic and ultramafic rocks of the high-Ti series (gabbroids of the Olenegorsk massif, xenoliths of ultramafic and mafic rocks in these gabbroids, and gabbroid veinlets in the xenoliths) were formed by tholeiite melts of the N-MORB type in an oceanic spreading center. The ultramafic and mafic rocks of the low-Ti series (dunite, pyroxenite, and gabbroid veinlets and bodies in the central and western parts of the peninsula) were produced by water-rich melts of the boninite type early in the course of suprasubductional magmatism.

3. Mineralogical and geochemical features of the plutonic ultramafic rocks, including their vein varieties, may provide natural evidence of an episode of boninite magmatism during the origin of ophiolite complexes.

4. Techniques used to evaluate the composition of melts trapped in ultramafic rocks and gabbroids make it possible to draw conclusions about the geodynamic

settings in which these rocks were formed and how much these rocks are cogenetic with spatially related basalts. These conclusions are more specified and justified than those based solely on the composition of the primary minerals of these rocks.

ACKNOWLEDGMENTS

The authors thank I.A. Roshchina†, T.G. Kuz'mina, T.V. Romashova, and Ya.V. Bychkova† for conducting the analytical work. The authors are grateful to E.V. Pushkarev (Zavaritsky Institute of Geology and Geochemistry, Ural Branch, Russian Academy of Sciences) for constructive criticism that led the authors to remarkably improve the manuscript.

FUNDING

This study was carried out under a government-financed research project for Vernadsky Institute of Geochemistry and Analytical Chemistry, Russian Academy of Sciences; the coauthors from other organizations of the Russian Academy of Sciences conducted this study under respective government-financed research projects for their institutions. The participation of D.P. Savelyev was supported by the Russian Science Foundation, project no. 22-27-00029.

CONFLICT OF INTEREST

The authors declare that they have no conflicts of interest.

SUPPLEMENTARY INFORMATION

The online version contains supplementary material available at https://doi.org/10.1134/S0869591123030025.

REFERENCES

Alexeiev, D.V., Gaedicke, C., Tsukanov, N.V., and Freitag, R., Collision of the Kronotskiy Arc at the NE Eurasia margin and structural evolution of the Kamchatka–Aleutian junction, *Int. J. Earth Sci.,* 2006, vol. 95, pp. 977–994.

Arai, S., Chemistry of chromian spinel in volcanic rocks as a potential guide to magma chemistry, *Mineral. Mag.,* 1992, vol. 56, pp. 173–184.

Arai, S., Okamura, H., Kadoshima, K., et al., Chemical characteristics of chromian spinel in plutonic rocks: implications for deep magma processes and discrimination of tectonic setting, *Isl. Arc,* 2011, vol. 20, no. 1, pp. 125–137.

Ariskin, A.A. and Barmina, G.S., COMAGMAT: development of a magma crystallization model and its petrological applications, *Geochem. Int.,* 2004, vol. 42, pp. 1–157.

Ballhaus, C., Berry, R.F., and Green, D.H., High pressure experimental calibration of the olivine-orthopyroxene-spinel oxygen geobarometer: implications for the oxidation state of the upper mantle, *Contrib. Mineral. Petrol.,* 1991, vol. 107, pp. 27–40.

Le Bas, M.J. and Streckeisen, A.L., The IUGS systematics of igneous rocks, *J. Geol. Soc.,* 1991, vol. 148, no. 5, pp. 825–833.

Batanova V.G., Lyaskovskaya Z.E., Savel'eva G.N., Sobolev A.V. Peridotites from the Kamchatsky Mys: evidence of oceanic mantle melting near a hotspot, *Russ. Geol. Geophys.,* 2014, vol. 55, no. 12, pp. 1395–1403.

Batanova, V.G., Belousov, I.A., Savelieva, G.N., and Sobolev, A.V., Consequences of channelized and diffuse melt transport in suprasubduction zone mantle: evidence from the Voykar ophiolite (Polar Urals), *J. Petrol.,* 2011, vol. 52, no. 12, pp. 2483–2521.

Bazylev, B.A., Ledneva, G.V., Bychkova, Ya.V., et al., Estimation of the content and composition of trapped melt in dunite, *Geochem. Int.*, 2019, vol. 64, no. 5, pp. 509–523.

Bédard, J.H., A procedure for calculating the equilibrium distribution of trace elements among the minerals of cumulate rocks, and the concentration of trace elements in the coexisting liquids, *Chem. Geol.,* 1994, vol. 118, pp. 143–153.

Bédard, J.H., Trace element partitioning in plagioclase feldspar, *Geochim. Cosmochim. Acta,* 2006, vol. 70, pp. 3717–3742.

Berger, J., Lo, K., Diot, H., et al., Deformation-driven differentiation during in situ crystallization of the 2.7 Ga Iguilid mafic intrusion (West African Craton, Mauritania), *J. Petrol.,* 2017, vol. 58, no. 4, pp. 819–840.

Betkhol'd, A.F., Kvasov, A.I., and Semenova, D.F., Geology, petrography, and geochemistry of ophiolites of the Kamchatsky Mys Peninsula (Eastern Kamchatka), *Tikhookean. Geol.,* 1986, no. 6, pp. 78–84.

Boyarinova, M.E., *Gosudarstvennaya geologicheskaya karta Rossiiskoi Federatsii m-ba 1 : 200 000. Seriya Vostochno-Kamchatskaya. Listy O-58-XXVI, XXXI, XXXII (Ust'-Kamchatsk)* (State Geological Map of the Russian Federation on a Scale 1 : 200 000. Eastern Kamchatka Seies. Sheets O-58-XXVI, XXXI, XXXII (Ust'-Kamchatsk)) St. Petersburg: VSEGEI, 1999.

Bragin, N.Yu., Zinkevich, V.P., Lyashenko, O.V., et al., *Middle Cretaceous (Aptian–Turonian) deposits in the tectonic structure of Eastern kamchatka, Ocherki po geologii Vostoka SSSR (Overview on Geology of Eastern USSR)*, Moscow: Nauka, 1986, pp. 21–34.

Dick, H.J.B. and Bullen, Th., Chromian spinel as a petrogenetic indicator in abyssal and alpine-type peridotites and spatially associated lavas, *Contrib. Mineral. Petrol.,* 1984, vol. 86, pp. 54–76.

Dilek, Y., *Ophiolite concept and its evolution, Ophiolite Concept and the Evolution of Geological Thought,* Dilek, Y., Newcomb, S., and Hawkins, J.W., Eds. *Geol. Soc. Am. Spec. Pap.,* 2003, vol. 373, pp. 1–16.

Dilek, Y. and Furnes, H., Ophiolite genesis and global tectonics: geochemical and tectonic fingerprinting of ancient oceanic lithosphere, *Geol. Soc. Am. Bull.,* 2011, vol. 123, nos. 3/4, pp. 387–411.

Duggen, S., Portnyagin, M., Baker, J., et al., Drastic shift in lava geochemistry in the volcanic-front to rear-arc region of the southern Kamchatkan subduction zone: evidence for the transition from slab surface dehydration to sediment melting, *Geochim. Cosmochim. Acta,* 2007, vol. 71, pp. 452–480.

Fedorchuk, A.V., Peyve, A.A., Gul'ko, N.I., and Savichev, A.T., Petrogeochemical types of basalts of ophiolite

association of the Kamchatka Mys Peninsula, Eastern Kamchatka, *Geokhimiya,* 1989, no. 12, pp. 1710–1717.

Frei, D., Liebscher, A., Franz, G., et al., Trace element partitioning between orthopyroxene and anhydrous silicate melt on the lherzolite solidus from 1.1 to 3.2 GPa and 1230 to 1535°C in the model system Na_2O–CaO–MgO–Al_2O_3–SiO_2, *Contrib. Mineral. Petrol.,* 2009, vol. 157, pp. 473–490.

Hawkins, J.W., *Geology of supra-subduction zones - implications for the origin of ophiolites, Ophiolite Concept and the Evolution of Geological Thought,* Dilek, Y., Newcomb, S., and Hawkins, J.W., Eds., *Geol. Soc. Am. Spec. Pap.,* 2003, vol. 373, pp. 227–268.

Hawthorne, F.C., Oberti, R., Harlow, G.E., et al., IMA report, nomenclature of the amphibole supergroup, *Am. Mineral.,* 2012, vol. 97, pp. 2031–2048.

Kamenetsky, V.S., Crawford, A.J., and Meffre, S., Factors controlling chemistry of magmatic spinel: an empirical study of associated olivine, Cr-spinel and melt inclusions from primitive rocks, *J. Petrol.,* 2001, vol. 42, no. 4, pp. 655–671.

Karimov, A.A., Gornova, M.A., Belyaev, V.A., et al., Genesis of pyroxenite veins in supra-subduction zone peridotites: evidence from petrography and mineral composition of Egiingol massif (northern Mongolia), *China Geol.,* 2020, vol. 3, no. 2, pp. 299–313.

Kelemen, P.B., Hanghøj, K., and Greene, A.R., One view of the geochemistry of subduction-related magmatic arcs, with an emphasis on primitive andesite and lower crust, *Treatise on Geochemistry,* Holland, H.D., Turekian, K.K., Eds., 2003, vol. 3, pp. 593–659.

Khotin, M.Yu. and Shapiro, M.N., Ophiolites of the Kamchatsky Mys Peninsula, Eastern Kamchatka: structure, composition, and geodynamic setting, *Geotectonics,* 2006, vol. 40, no.4, pp. 297–320.

Korneeva, A.A., Nekrylov, N., Kamenetsky, V.S., et al., Composition, crystallization conditions and genesis of sulfide-saturated parental melts of olivine-phyric rocks from Kamchatsky Mys (Kamchatka, Russia), *Lithos,* 2020, vol. 370–371, p. 105657.

Kramer, V., Skolotnev, S.G., Tsukanov, N.V., et al., Geochemistry, mineralogy, and geological position of mafic-ultramafic complexes of the Kamchatsky Mys Peninsula: preliminary results, *Petrologiya i metallogeniya bazit-giperbazitovykh kompleksov Kamchatki* (Petrology and Metallogeny of Mafic–Ultramafic Complexes of Kamchatka), Moscow: Nauchnyi mir, 2001, pp. 170–191.

Lander, A.V. and Shapiro, M.N., *The origin of the modern Kamchatka subduction zone*, Eichelberger, J., Gordeev, E., Izbekov, P., Eds., *Geophys. Monogr. Ser.,* 2007, vol. 172, pp. 57–64.

Ledneva, G.V., Bazylev, B.A., Kuzmin, D.V., and Kononkova, N.N., Pyroxenite veins in spinel peridotites of the Unnavayam sheet, Kuyul Ophiolite Terrane (Koryak Upland): origin and setting of formation, *Geochem. Int.,* 2017, vol. 55, no. 4, pp. 330–340.

Levashova, N.M., Shapiro, M.N., Ben'yamovskii, V.N., and Bazhenov, M.L., Kinematics of the Kronotskii Island Arc (Kamchatka) from paleomagnetic and geological data, *Geotectonics*, 2000, vol. 34, no. 2, pp. 141–159.

Locock, A.J., An Excel spreadsheet to classify chemical analyses of amphiboles following the IMA 2012 recommendations, *Comp. Geosci.*, 2014, vol. 62, pp. 1–11.

Luchitskaya, M.V., Tsukanov, N.V., and Skolotnev, S.G., New SHRIMP U–Pb age data on zircons from plagiogranites in the ophiolites of the Kamchatsky Mys Peninsula, Eastern Kamchatka, *Dokl. Earth Sci.,* 2006, vol. 408, no. 4, pp. 535–537.

Nekrylov, H. Korneeva, A.A., Savelyev, D.P., and Antsiferova, T.N., Variations of source composition and melting degrees of olivine-phyric rocks from Kamchatsky Mys: results of geochemical modeling of trace element contents in melts, *Petrology,* 2021, vol. 29, no. 1, pp. 14–23.

Osipenko, A.B. and Krylov, K.A., Geochemical heterogeneity of mantle peridotites in ophiolites of Eastern Kamchatka: reasons and geodynamic consequences, *Petrologiya i metallogeniya bazit-giperbazitovykh kompleksov Kamchatki* (Petrology and Metallogeny of Mafic–Ultramafic Complexes of Kamchatka), Moscow: Nauchnyi mir, 2001, pp. 138–158.

Parkinson, I.J. and Pearce, J.A., Peridotites from the Izu–Bonin–Mariana forearc (ODP Leg 125): evidence for mantle melting and melt-mantle interaction in a supra-subduction zone setting, *J. Petrol.,* 1998, vol. 39, no. 9, pp. 1577–1618.

Peyve, A.A., Ultramafic rocks of the Kamchatsky Mys Peninsula (Eastern Kamchatka), *Tikhookean. Geol.,* 1987, no. 2, pp. 41–46.

Perk, N.W., Coogan, L.A., Karson, J.A., et al., Petrology and geochemistry of primitive lower oceanic crust from Pito Deep: implications for the accretion of the lower crust at the southern East Pacific Rise, *Contrib. Mineral. Petrol.,* 2007, vol. 154, pp. 575–590.

Portnyagin, M.V., Origin of Suprasubduction Mantle Magmas by the Example of the Troodos Ophiolite Complex, Cyprus Island, *Extended Abstract of Candidate's (Geol.-Min.) Dissertation* (GEOKHI, Moscow, 1997).

Portnyagin, M., Hoernle, K., Hauff, F., et al., New data of Cretaceous Pacific MORB from accretionary complexes in Kamchatka: implications for the origin of depleted component in the hawaiian hotspot lavas, *Geophys. Res. Abs.,* 2006, vol. 8, p. 04937.

Portnyagin, M.V., Savelyev, D.P., Hoernle, K., et al., Mid-Cretaceous Hawaiian tholeiites preserved in Kamchatka, *Geology,* 2008, vol. 36, no. 11, pp. 903–906.

Portnyagin, M., Hoernle, K., and Savelyev, D., Ultra-depleted melts from Kamchatkan ophiolites: evidence for the interaction of the Hawaiian plume with an oceanic spreading center in the Cretaceous?, *Earth Planet. Sci. Lett.,* 2009, vol. 287, pp. 194–204.

Raznitsin, Yu.N., Khubunaya, S.A., and Tsukanov, N.V., Tectonics of eastern Kronotsky Peninsula and formation affiliation of basalts, *Geotektonika,* 1985, no. 1, pp. 88–101.

Ridolfi, F., Renzulli, A., and Puerini, M., Stability and chemical equilibrium of amphibole in calc-alkaline magmas: an overview, new thermobarometric formulations and application to subduction-related volcanoes, *Contrib. Mineral. Petrol.,* 2010, vol. 160, pp. 45–66.

Savelyev, D.P., Within-plate alkaline basalts in the Cretaceous accretionary complex of the Kamchatka Peninsula (Eastern Kamchatka), *Vulkanol. Seismol.,* 2003, no. 1, pp. 14–20.

Shcherbinina, E.A., Nannoplankton from Paleogene deposits in Eastern Kamchatka, *Stratigraphy. Geol. Correlation,* 1997, vol. 5, no. 2, pp. 156–166.

Skolotnev, S.G., Tsukanov, N.V., Savelyev D.P., and Fedorchuk, A.V., Compositional heterogeneity of the island-arc rocks of the Kronotsky and Kamchatsky Mys segments of the Kronotsky paleoarc, Kamchatka, *Dokl. Earth Sci.,* 2008, vol. 418, no. 1, pp. 37–41.

Sobolev, A.V. and Nikogosyan, I.K., Petrology of magmatism of long-term mantle jets: Hawaiian Islands (Pacific Ocean) and Reunion Island (Indian Ocean), *Petrologiya,* 1994, no. 2, pp. 131–168

Sobolev, A.V. and Danyushevsky, L.V., Petrology and geochemistry of boninites from the north termination of the Tonga trench: constraints on the generation conditions of primary high-ca boninite magmas, *J. Petrol.,* 1994, vol. 35, no. 5, pp. 1183–1211.

Sobolev, A.V. and Shaussidon, M., H_2O concentrations in primary melts from supra-subduction zones and mid-ocean ridges: implications for H_2O storage and recycling in the mantle, *Earth Planet. Sci. Lett.,* 1996, vol. 137, no. 1, pp. 45–55.

Sun, S.S. and McDonough, W.F., *Chemical and isotopic systematics of oceanic basalts: implication for mantle composition and processes, Magmatism in the Oceanic Basins,* Saunders, A.D. and Norry, M.J., Eds., *Geol. Soc. Spec. Publ,* 1989, vol. 42, pp. 313–345.

Tamura, A. and Arai, S., Harzburgite–dunite–orthopyroxenite suite as a record of supra-subduction zone setting for the Oman ophiolite mantle, *Lithos,* 2006, vol. 90, nos. 1–2, pp. 43–56.

Tsukanov, N.V., Palechek, T.N., Soloviev, A.V., and Savelyev, D.P., Tectonostratigraphic complexes of the southern Kronotskii Paleoarc (Eastern Kamchatka): structure, age, and composition, *Russ. J. Pac. Geol.,* 2014, vol. 8, no. 4, pp. 233–246.

Tsukanov, N.V., Kramer, W., Skolotnev, S.G., et al., Ophiolites of the eastern peninsulas zone (Eastern Kamchatka): age, composition, and geodynamic diversity, *Island Arc,* 2007, vol. 16, no. 3, pp. 431–456.

Varfalvy, V., Hebert, R., Bedard, J.H., and Lafleche, M.R., Petrology and geochemistry of pyroxenite dykes in upper mantle peridotites of the North Arm mountain massif, bay of islands ophiolite, Newfoundland: implications for the genesis of boninitic and related magmas, *Can. Mineral.,* 1997, vol. 35, no. 2, pp. 543–570.

Vysotskii, S.V., *Ofiolitovye assotsiatsii ostrovoduzhnykh sistem Tikhogo okeana* (Ophiolite Associations of the Pacific Island-Arc Systems), Vladivostok: DVO AN SSSR, 1986.

Warr, L.N., IMA-CNMNC approved mineral symbols, *Mineral. Mag.,* 2021, vol. 85, pp. 291–320.

Zajacz, Z. and Halter, W., LA-ICPMS analyses of silicate melt inclusions in co-precipitated minerals: quantification, data analysis and mineral/melt partitioning, *Geochim. Cosmochim. Acta,* 2007, vol. 71, pp. 1021–1040.

Zinkevich V.P., Konstantinovskaya E.A., Tsukanov N.V., et al., *Akkretsionnaya tektonika Vostochnoi Kamchatki* (Accretionary Tectonics of Eastern Kamchatka), Moscow: Nauka, 1993.

Zinkevich, V.P. and Tsukanov, N.V., Formation of accrcetionary structure of Eastern Kamchatka in the Late Mesozoic–Early Cenozoic, *Geotektonika,* 1992, no. 4, pp. 97–112.

Translated by E. Kurdyukov